The Chirality-Flow Method for Massive and Electroweak Amplitudes

Joakim Alnefjord

Department of Astronomy and Theoretical Physics, Lund University

LUND UNIVERSITY

Abstract

In this thesis I extend the chirality-flow method to the full standard model at tree-level by including massive particles and electroweak interactions. The chirality-flow method is a new diagrammatic method for calculating Feynman diagrams that is based on the spinor-helicity formalism, that before this thesis was written had been worked out for massless QED and QCD at tree-level. I summarize what is known about massive spinor-helicity calculations and use this as the basis for the extended diagrammatic interpretation for massive particles. I use the Lorentz structure of the electroweak vertices to rewrite them in the chirality-flow picture.

Populärvetenskaplig beskrivning

Det finns många vägar att gå i jakten efter en bättre förståelse för vår materiella världs minsta beståndsdelar, elementarpartiklarna. Vi kan bygga kraftigare och mer exakta partikelacceleratorer och därmed förbättra den experimentella delen av partikelfysiken. Vi kan också försöka hitta nya teorier om hur världen fungerar, något som i praktiken är väldigt komplicerat. Vi kan istället fokusera på smartare sätt att göra uträkningar inom dagens teoretiska ramar, vilket är vad den här uppsatsen handlar om.

Inom partikelfysiken är vi ofta intresserade av att räkna ut så kallade övergångsamplituder. Dessa kan exempelvis liknas med en sannolikhet att ett visst tillstånd av partiklar ska övergå till ett annat tillstånd av andra partiklar vid en kollision i partikelacceleratorer. För det mesta har vi inget exakt svar för övergångsamplituderna, så istället approximeras dem. Målet är att försöka göra så bra approximationer som möjligt.

Ofta används en typ av diagram, som kallas för Feynman diagram efter nobelpristagande fysikern Richard Feynman, för att hjälpa till i beräkningarna. Diagram är ett smidigt sätt att lättare visualisera uträkningarna och det finns flera typer av diagram som används. Nu har vi en ny metod som kallas för "chirality-flow method" med en ny typ av diagram som förhoppningsvis ska kunna göra uträkningar lättare. Den här nya metoden har utvecklats för att kunna appliceras på vissa av elementarpartiklarna, där partiklarnas massa också har ignorerats. Målet med den här uppsatsen är att inkludera alla typer av kända elementarpartiklar samt deras massa, så att den nya metoden kan appliceras i alla möjliga fall.

Acknowledgments

Contents

1   Introduction

In particle physics we are often interested in scattering amplitudes which are needed to calculate cross sections. The complexity of the calculations increases not only from loops in higher order terms of the perturbation series, but also when we increase the number of external particles involved in a specific process. To counter the complexity of calculations, we would like to have better and more efficient methods of calculating the scattering amplitudes, which will help us increase the accuracy of our theoretical predictions.

The chirality-flow method [1] is a new diagrammatic method for calculating scattering amplitudes, which has been developed for amplitude calculations for massless QED and QCD at tree-level. It is based on the spinor-helicity formalism [2, 3, 4, 5, 6] where objects used in amplitude calculations such as Dirac spinors, Feynman-slashed momenta, and polarization vectors are all decomposed and written in terms of two-component Weyl spinors [7]. The chirality-flow method interprets the Weyl spinor inner products as flow lines in chirality-flow diagrams. These flow diagrams are very powerful because they drastically simplify calculations.

In this thesis, I have generalised the chirality-flow method to also include masses and the electroweak sector, so that it can be used for the full Standard Model at tree-level. This has been achieved by using what is known about massive spinor-helicity calculations and including that in the diagrammatic framework of the chirality-flow formalism. I find that massive Feynman diagrams with a specific helicity configuration can be decomposed into sums of massless chirality-flow diagrams, which allows us to apply the tools that have been developed for the massless chirality-flow method.

Before we begin, I will give a brief overview of the thesis. In section 2, I start with the representations of the Lorentz group and how objects involved in Feynman diagrams can be written in terms of two-component Weyl spinors using the spinor-helicity formalism. Then in section 3 I summarise how this formalism can be used to create a diagrammatic method, called the chirality-flow method, which has been recently developed for massless QED and QCD at tree-level. In section 4 I use what is known about massive spinor-helicity calculations to put it into a form which can be inserted into the chirality-flow framework. I then in section 5 describe how massive particles can be interpreted and used diagrammatically, and I also give chirality-flow rules for the electroweak vertices. Lastly in section 6 I show some examples of the diagrammatic method being used.

2   Background

We will begin with brief summaries of two components that lie at the core of the chirality-flow method: the Lorentz group and the spinor-helicity formalism. These two parts will be used as the starting points for the description of the chirality-flow method.

2.1 The Lorentz Group

The Lorentz group [8] describes Lorentz transformations in Minkowski-space and it has 6 generators: 3 rotation generators J_i and 3 boost generators K_i. The generators satisfy the following commutation relations:

$$[J_i, J_j] = i\epsilon_{ijk}J_k, \quad [J_i, K_j] = i\epsilon_{ijk}K_k, \quad [K_i, K_j] = -i\epsilon_{ijk}J_k. \tag{2.1}$$

Together, the generators and commutation relations describe the Lie algebra of the Lorentz Group. It is possible to define a new set of operators as combinations of the rotation and boost generators,

$$N_i^{\pm} = \frac{1}{2}\left(J_i \pm iK_i\right), \tag{2.2}$$

which gives us a new set of commutation relations:

$$\left[N_i^+, N_j^+\right] = i\epsilon_{ijk}N_k^+, \quad \left[N_i^-, N_j^-\right] = i\epsilon_{ijk}N_k^-, \quad \left[N_i^+, N_j^-\right] = 0. \tag{2.3}$$

We see here that N_i^+ and N_i^- form two copies of $\mathfrak{su}(2)_{\mathbb{C}}$ Lie algebras that commute with each other. The Lie algebra isomorphism $\mathfrak{so}(3,1)_{\mathbb{C}} \simeq \mathfrak{su}(2)_{\mathbb{C}} \oplus \mathfrak{su}(2)_{\mathbb{C}}$ is a more formal way to display this. This isomorphism between Lie algebras can be used to characterize the irreducible representations of the Lorentz Group as (s_1, s_2), where $s_1, s_2 = 0, \frac{1}{2}, 1, \frac{3}{2}, ...$ give the specific irreducible representations of the two copies of $\mathfrak{su}(2)_{\mathbb{C}}$.

Some examples of common representations are:

- The scalar representation is given by $(0,0)$, where both copies of $\mathfrak{su}(2)_{\mathbb{C}}$ are given in the trivial representation.

- Left-chiral and right-chiral Weyl spinors are 2-component spinors that transform under the $(\frac{1}{2}, 0)$-representation and the $(0, \frac{1}{2})$-representation, respectively.

- Dirac spinors are 4-component spinors that are formed by combining a left-chiral and a right-chiral Weyl spinor, and they transform under the $(\frac{1}{2}, 0) \oplus (0, \frac{1}{2})$-representation.

- The $(\frac{1}{2}, \frac{1}{2})$-representation is the vector representation. We use this to represent a vector object as a product of a left-chiral and a right-chiral Weyl spinor.

2.2 The Spinor-Helicity Formalism

There are two parts that lie at the core of the spinor-helicity formalism: the use of 2-component Weyl spinors and the use of the helicity basis. Dirac spinors, Feynman-slashed momenta, and polarization vectors can all be written in terms of Weyl spinors. Using these spinors, it is possible to form two types of Weyl spinor contractions that are Lorentz invariant, which is usually helpful and appreciated. The helicity basis is a good choice for

a spin basis, as the helicity operator commutes with the Dirac Hamiltonian, which means that their eigenstates are the same. The use of helicity is especially useful for massless particles because it is then Lorentz invariant, whereas for massive particles helicity is frame dependent.

Since we are working with Weyl spinors, we use the Weyl/chiral basis for the gamma matrices,

$$\gamma^\mu = \begin{pmatrix} 0 & \sigma^\mu \\ \bar{\sigma}^\mu & 0 \end{pmatrix} = \begin{pmatrix} 0 & \sqrt{2}\tau^\mu \\ \sqrt{2}\bar{\tau}^\mu & 0 \end{pmatrix}, \quad \sigma^\mu = \left(1, \sigma^i\right), \quad \bar{\sigma}^\mu = \left(1, -\sigma^i\right), \quad (2.4)$$

where σ^i are the Pauli matrices:

$$\sigma^1 = \begin{pmatrix} 0 & 1 \\ 1 & 0 \end{pmatrix}, \quad \sigma^2 = \begin{pmatrix} 0 & -i \\ i & 0 \end{pmatrix}, \quad \sigma^3 = \begin{pmatrix} 1 & 0 \\ 0 & -1 \end{pmatrix}. \quad (2.5)$$

We write the σ-matrices as $\sqrt{2}\tau^\mu$ to avoid having to carry around unnecessary factors of 2 through the calculations. For the τ-matrices we have the relation

$$g^{\mu\nu} = \text{Tr}\left(\tau^\mu \bar{\tau}^\nu\right) = \bar{\tau}^\mu_{\alpha\dot{\beta}} \tau^{\nu,\dot{\beta}\alpha} = \tau^{\mu,\dot{\alpha}\beta} \bar{\tau}^\nu_{\beta\dot{\alpha}}, \quad (2.6)$$

where the α and β indices will be explained further in section 3.1, without a factor of 2 that would have been included if σ matrices were used instead. The chiral projection operators P_L and P_R also take on a diagonal form in the chiral basis:

$$\gamma^5 \equiv i\gamma^0\gamma^1\gamma^2\gamma^3 = \begin{pmatrix} -1 & 0 \\ 0 & 1 \end{pmatrix}, \quad P_L \equiv \frac{1}{2}\left(1 - \gamma^5\right) = \begin{pmatrix} 1 & 0 \\ 0 & 0 \end{pmatrix}, \quad P_R \equiv \frac{1}{2}\left(1 + \gamma^5\right) = \begin{pmatrix} 0 & 0 \\ 0 & 1 \end{pmatrix}. \quad (2.7)$$

We can use bras and kets to represent the Weyl spinors: square bra-kets, $[p|$ and $|p]$, represent left-chiral Weyl spinors and angled bra-kets, $\langle p|$ and $|p\rangle$, represent right-chiral Weyl spinors. The square and angled bracket spinors are related by hermitian conjugation,

$$|p]^\dagger = \langle p|, \quad |p\rangle^\dagger = [p|. \quad (2.8)$$

More specifically, $[p|$ and $\langle p|$ are 2-component complex row vectors, while $|p]$ and $|p\rangle$ are 2-component complex column vectors. We can use these to form antisymmetric spinor contractions as

$$[p_i p_j] = -[p_j p_i] \quad \text{and} \quad \langle p_i p_j\rangle = -\langle p_j p_i\rangle, \quad (2.9)$$

both of which are Lorentz invariant complex numbers. It is in principle possible to form contractions with spinors of opposite type, but these will not be Lorentz invariant quantities.

We will now briefly look at how Dirac spinors, Feynman-slashed momenta, and polarization vectors can all be written in terms of Weyl spinors. Dirac spinors transform under the

3

$(\frac{1}{2}, 0) \oplus (0, \frac{1}{2})$-representation and can therefore be written in terms of Weyl spinors, here shown in a generic form with its Dirac conjugate:

$$\Psi = \begin{pmatrix} |\alpha] \\ |\beta\rangle \end{pmatrix}, \quad \overline{\Psi} = \Psi^\dagger \gamma^0 = \left(|\beta\rangle^\dagger \quad |\alpha]^\dagger \right) = \left([\beta| \quad \langle\alpha| \right), \tag{2.10}$$

where $|\alpha]$ and $|\beta\rangle$ are left- and right-chiral Weyl spinors, respectively. For a massive fermion both chiralities contribute to a specific helicity state and it is possible to perform a Lorentz boost to a different reference frame where the helicity is the opposite. However, the Dirac spinor becomes particularly simple in the massless limit as one of the two Weyl spinors goes to zero. Which one goes to zero depends on the specific helicity of the particle. This is because for massless fermions helicity and chirality are in a one-to-one relationship, meaning that a specific chirality only contributes to one of the two helicities. It is also not possible to perform a Lorentz boost to change the helicity of the fermion in the massless case.

The projection operators in eq. (2.7) simply project out the left- and right-chiral components of the Dirac spinor:

$$P_L \Psi = \begin{pmatrix} |\alpha] \\ 0 \end{pmatrix}, \quad P_R \Psi = \begin{pmatrix} 0 \\ |\beta\rangle \end{pmatrix}. \tag{2.11}$$

Four-currents and other objects can be split into parts in the chiral basis. An example of this splitting is:

$$\overline{v} \gamma^\mu u = \begin{pmatrix} v_R^\dagger & v_L^\dagger \end{pmatrix} \begin{pmatrix} 0 & \sqrt{2}\tau^\mu \\ \sqrt{2}\overline{\tau}^\mu & 0 \end{pmatrix} \begin{pmatrix} u_L \\ u_R \end{pmatrix} = \sqrt{2} v_R^\dagger \tau^\mu u_R + \sqrt{2} v_L^\dagger \overline{\tau}^\mu u_L, \tag{2.12}$$

where we have written the two Dirac spinors $\overline{v}$ and u in terms of their left- and right-chiral components.

Feynman-slashed momenta $\slashed{p}_\gamma = p_\mu \gamma^\mu$ coming from the, for now massless, fermion propagators $\dfrac{i\slashed{p}_\gamma}{p^2}$ can also be decomposed into Weyl spinors. In the chiral basis we have

$$\slashed{p}_\gamma = \begin{pmatrix} 0 & \slashed{p}_\sigma \\ \slashed{p}_{\overline{\sigma}} & 0 \end{pmatrix} = \begin{pmatrix} 0 & p_\mu \sigma^\mu \\ p_\mu \overline{\sigma}^\mu & 0 \end{pmatrix}. \tag{2.13}$$

For a p^μ where $p^2 = 0$, it is possible to decompose both $\slashed{p}_\sigma$ and $\slashed{p}_{\overline{\sigma}}$ into products of Weyl spinors:

$$\slashed{p}_\sigma = |p]\langle p|, \quad \slashed{p}_{\overline{\sigma}} = |p\rangle[p]. \tag{2.14}$$

This can also be applied for each individual p_i^μ where $p^\mu = \sum_i p_i^\mu$ and $p_i^2 = 0$ for all i. More about this and the generalisation to massive particles will be described in section 4.1.

Finally, polarization vectors transform under the $(\frac{1}{2}, \frac{1}{2})$-representation, which is the product of the left- and right-chiral representations $(\frac{1}{2}, 0) \otimes (0, \frac{1}{2})$, and can be written in terms of

4

Weyl spinors as

$$\varepsilon_+^\mu(p) = \frac{[q|\tau^\mu|p\rangle}{[pq]} \quad \text{and} \quad \varepsilon_-^\mu(p) = \frac{[p|\tau^\mu|q\rangle}{\langle qp \rangle}, \tag{2.15}$$

where q is a light-like reference momentum and where we for simplicity only include the two massless polarization states.

3 The Massless Chirality-Flow Method

The chirality-flow method is a new method for calculating transition amplitudes, and it was created as a diagrammatic method on top of the spinor-helicity and Weyl-van-der-Waerden (WvdW) formalisms. Using this method it is easy to move from a Feynman diagram, to one or more chirality-flow diagrams, to complex numbers in terms of Lorentz invariant spinor contractions. The flow diagrams make it trivial to keep track of the spinor contractions used in the spinor-helicity and WvdW formalisms.

3.1 Notation and Diagrammatic Interpretation

All objects described in the previous section can be given an index structure using the Weyl-van-der-Waerden formalism [9]. We begin with Weyl spinors. Left-chiral column spinors are given upper dotted indices, $|p] \leftrightarrow \tilde{\lambda}_p^{\dot\alpha}$, and right-chiral column spinors are given lower undotted indices, $|p\rangle \leftrightarrow \lambda_{p,\alpha}$, where we for now use λ for the undotted spinors and $\tilde{\lambda}$ for the dotted spinors. Hermitian conjugation is used to add or remove a dot over an index which gives us the row spinors:

$$(\lambda_\alpha)^\dagger = \tilde{\lambda}_{\dot\alpha}, \quad \left(\tilde{\lambda}^{\dot\alpha}\right)^\dagger = \lambda^\alpha. \tag{3.1}$$

We can use the antisymmetric tensor ϵ as a metric for the spinors, in the form of $\epsilon^{\alpha\beta}$, $\epsilon^{\dot\alpha\dot\beta}$, $\epsilon_{\alpha\beta}$, or $\epsilon_{\dot\alpha\dot\beta}$, to raise or lower dotted and undotted indices, where $\epsilon^{12} = -\epsilon^{21} = \epsilon_{21} = -\epsilon_{12} = 1$ and other elements are zero. We have:

$$\lambda^\alpha = \epsilon^{\alpha\beta}\lambda_\beta, \quad \tilde{\lambda}^{\dot\alpha} = \epsilon^{\dot\alpha\dot\beta}\tilde{\lambda}_{\dot\beta}, \quad \lambda_\alpha = \epsilon_{\alpha\beta}\lambda^\beta, \quad \tilde{\lambda}_{\dot\alpha} = \epsilon_{\dot\alpha\dot\beta}\tilde{\lambda}^{\dot\beta}. \tag{3.2}$$

Using ϵ as a metric, we can form Lorentz invariant spinor contractions or spinor inner products, and these can be drawn as diagrams. The *undotted* indices are related to *undotted* lines and angled brackets, and *dotted* indices to *dotted* lines and square brackets. We have:

$$\langle p_i p_j \rangle = \langle ij \rangle = \lambda_i^\alpha \lambda_{j,\alpha} = \epsilon^{\alpha\beta}\lambda_{i,\beta}\lambda_{j,\alpha} = \quad i \longrightarrow j \quad , \tag{3.3a}$$

$$[p_i p_j] = [ij] = \tilde{\lambda}_{i,\dot\alpha}\tilde{\lambda}_j^{\dot\alpha} = \epsilon_{\dot\alpha\dot\beta}\tilde{\lambda}_i^{\dot\beta}\tilde{\lambda}_j^{\dot\alpha} = \quad i \text{ -----} \blacktriangleright \text{----- } j \quad , \tag{3.3b}$$

$$\langle ij \rangle = [ji]^*, \quad \langle ij \rangle = -\langle ji \rangle, \quad \text{and} \quad [ij] = -[ji]. \tag{3.3c}$$

We note that undotted indices are contracted from upper to lower, dotted indices from lower to upper, and that the arrow points from the first particle index to the second. The direction of the arrow is important as these are both antisymmetric contractions, because of the antisymmetry of ϵ.

The spinor contractions may also be written using Kronecker deltas as $\lambda_i^\alpha \lambda_{j,\alpha} = \lambda_i^\alpha \delta_\alpha{}^\beta \lambda_{j,\beta}$ or $\tilde{\lambda}_{i,\dot{\alpha}} \tilde{\lambda}_j^{\dot{\alpha}} = \tilde{\lambda}_{i,\dot{\alpha}} \delta^{\dot{\alpha}}{}_{\dot{\beta}} \tilde{\lambda}_j^{\dot{\beta}}$ where we may choose to define

$$\delta_\alpha{}^\beta = \quad\overrightarrow{}_{\alpha \qquad \beta} \quad \text{and} \quad \delta^{\dot{\alpha}}{}_{\dot{\beta}} = \quad\overrightarrow{}_{\dot{\alpha} \qquad \dot{\beta}} \tag{3.4}$$

For massless fermions, when helicity and chirality are in a one-to-one relationship, a single two-component Weyl spinor is enough to describe a fermion of a specific helicity. A left-chiral Weyl spinor describes an outgoing positive helicity fermion or anti-fermion, and a right-chiral Weyl spinor describes an outgoing negative helicity fermion or anti-fermion. In this thesis all particles are considered outgoing. The four types of outgoing fermions/anti-fermions and the relations between indices, brackets, Feynman diagrams, and chirality-flow diagrams are:

Right-chiral fermion: $\quad\lambda_i^\alpha \leftrightarrow \langle i | = \bigcirc\!\!\longrightarrow\!\!\frac{i}{-} = \bigcirc\!\!\longleftarrow\!\! i \quad,\quad$ (3.5a)

Right-chiral anti-fermion: $\lambda_{i,\alpha} \leftrightarrow | i \rangle = \bigcirc\!\!\longleftarrow\!\!\frac{i}{-} = \bigcirc\!\!\longrightarrow\!\! i \quad,\quad$ (3.5b)

Left-chiral fermion: $\quad\tilde{\lambda}_{i,\dot{\alpha}} \leftrightarrow [i | = \bigcirc\!\!\longrightarrow\!\!\frac{i}{+} = \bigcirc\!\!\dashleftarrow\!\! i \quad,\quad$ (3.5c)

Left-chiral anti-fermion: $\quad\tilde{\lambda}_i^{\dot{\alpha}} \leftrightarrow | i] = \bigcirc\!\!\longleftarrow\!\!\frac{i}{+} = \bigcirc\!\!\dashrightarrow\!\! i \quad.\quad$ (3.5d)

Note that the direction of the arrows in the chirality-flow diagrams are defined opposite to the direction of the Feynman diagram arrows.

If we for a massless four-vector p^μ use light-cone coordinates $p^\pm = p^0 \pm p^3$ and $p^\perp = p^1 + ip^2$ we can write its Weyl spinors as [1]

$$\lambda_p^\alpha \leftrightarrow \langle p | = \frac{1}{\sqrt{p^+}} \left(p^\perp \quad -p^+ \right), \quad \lambda_{p,\alpha} \leftrightarrow | p \rangle = \frac{1}{\sqrt{p^+}} \begin{pmatrix} p^+ \\ p^\perp \end{pmatrix},$$

$$\tilde{\lambda}_{p,\dot{\alpha}} \leftrightarrow [p | = \frac{1}{\sqrt{p^+}} \left(p^+ \quad p^{\perp *} \right), \quad \tilde{\lambda}_p^{\dot{\alpha}} \leftrightarrow | p] = \frac{1}{\sqrt{p^+}} \begin{pmatrix} p^{\perp *} \\ -p^+ \end{pmatrix}. \tag{3.6}$$

The Weyl-van-der-Waerden notation imposed on eq. (2.12) implies an index structure for the τ matrices, used in $ff\gamma$ (fermion-fermion-photon) and ffg (fermion-fermion-gluon)

6

vertices, which diagrammatically looks like

$$\tau^\mu \leftrightarrow \tau^{\mu,\dot\alpha\beta} = \quad\quad\quad \text{and} \quad \bar\tau^\mu \leftrightarrow \bar\tau^\mu_{\alpha\dot\beta} = \quad\quad\quad , \tag{3.7}$$

where the photon line may also be replaced by a gluon line.

If a massless external particle is given a specific helicity, then that corresponds to a specific chirality, which means that only one of the two matrices above will contribute to a vertex. If an outgoing positive helicity particle is connected to a $ff\gamma$ or ffg vertex, then only the flow diagram in which that particle line is dotted contributes to the amplitude, and for outgoing negative helicity particles, only undotted lines contribute. This also means that if two outgoing massless fermions are connected to the same $ff\gamma$ or ffg vertex, then they need to have opposite helicities for the amplitude to be non-zero. An example in the massless case is

$$\quad = ieQ_f\sqrt{2} \quad\quad = ieQ_f\sqrt{2}\tilde\lambda_{i,\dot\alpha}\tau^{\mu,\dot\alpha\beta}\lambda_{j,\beta} = ieQ_f\sqrt{2}[i|\tau^\mu|j\rangle,$$

$$\tag{3.8}$$

where the factors in front of the second diagram come from the $ff\gamma$ vertex and the fermion lines have been translated using eq. (3.5). In this same line we see how the expression can also be written in index form or bra-ket form.

The fermion propagator contains a factor of $\not{p}_\gamma = p_\mu\gamma^\mu$ which in the chiral basis looks like

$$\not{p}_\gamma = \begin{pmatrix} 0 & \not{p}_\sigma \\ \not{p}_{\bar\sigma} & 0 \end{pmatrix}, \tag{3.9}$$

where the subscript indicates what matrix p^μ has been contracted with. From here on, $\not{p}_\sigma$ and $\not{p}_{\bar\sigma}$ will simply be referred to as $\not{p}$ and $\bar{\not{p}}$, respectively. For the determinants we have $\det\left(\not{p}\right) = \det\left(\bar{\not{p}}\right) = p^2$ which is zero in the massless case. If the determinant of a 2x2 matrix is zero, then it can be decomposed into an outer product of two vectors, or in this case two Weyl spinors, so that $\sqrt{2}p^{\dot\alpha\beta} = \tilde\lambda_p^{\dot\alpha}\lambda_p^\beta = |p]\langle p|$ and $\sqrt{2}p_{\alpha\dot\beta} = \lambda_{p,\alpha}\tilde\lambda_{p,\dot\beta} = |p\rangle[p|$. The reason for this decomposition is to make it possible to form spinor contractions as $\langle ij\rangle$ or $[ij]$. For $\not{p}$ and $\bar{\not{p}}$ we have

$$\not{p} = \sqrt{2}p_\mu\tau^\mu \leftrightarrow \sqrt{2}p^{\dot\alpha\beta} = \quad , \quad \bar{\not{p}} = \sqrt{2}p_\mu\bar\tau^\mu \leftrightarrow \sqrt{2}\bar p_{\alpha\dot\beta} = \quad ,$$

$$\tag{3.10}$$

where in both diagrams the arrows point in the direction of the index order, meaning that in the first diagram they point from $\dot\alpha$ to β, and in the second diagram they point from α to $\dot\beta$.

7

We also have for p^μ [1]:

$$\sqrt{2}p^\mu \leftrightarrow \quad p \; \bullet\!\!-\!\!-\!\!-\!\!-\!\!\diagdown \quad , \tag{3.11}$$

which will be used for the triple gluon vertex in eq. (3.25) and the triple electroweak vector boson vertex in eq. (5.15).

A 4-vector p^μ can be written in bispinor form, where

$$\sqrt{2}p^{\dot\alpha\beta} = \sqrt{2}p^\mu \tau_\mu^{\dot\alpha\beta} = p^\mu \sigma_\mu^{\dot\alpha\beta} \leftrightarrow \not{p} = \begin{pmatrix} p^0 - p^3 & -p^1 + ip^2 \\ -p^1 - ip^2 & p^0 + p^3 \end{pmatrix} \tag{3.12a}$$

and

$$\sqrt{2}\bar{p}_{\alpha\dot\beta} = \sqrt{2}p^\mu \bar{\tau}_{\mu,\alpha\dot\beta} = p^\mu \bar{\sigma}_{\mu,\alpha\dot\beta} \leftrightarrow \bar{\not{p}} = \begin{pmatrix} p^0 + p^3 & p^1 - ip^2 \\ p^1 + ip^2 & p^0 - p^3 \end{pmatrix}. \tag{3.12b}$$

We can also use eq. (2.6) to get back the 4-vector we started with:

$$p^\mu = p^{\dot\alpha\beta}\bar{\tau}^\mu_{\beta\dot\alpha} = \bar{p}_{\alpha\dot\beta}\tau^{\mu,\dot\beta\alpha}. \tag{3.13}$$

The scalar product between two 4-vectors p^μ_i and p^μ_j can be represented diagrammatically as

$$2p_i \cdot p_j = 2p^\mu_i p^\nu_j \mathrm{Tr}(\tau_\mu\bar{\tau}_\nu) = \mathrm{Tr}(\not{p}_i\bar{\not{p}}_j) = \sqrt{2}p^{\dot\alpha\beta}_i\sqrt{2}\bar{p}_{j,\beta\dot\alpha} = \begin{matrix} p_i \\ \bullet \\ \Big(\Big) \\ \bullet \\ p_j \end{matrix}. \tag{3.14}$$

The 4-momentum p^μ going through the propagator can always be written as a sum of 4-momenta p^μ_k where each individual p^μ_k satisfies $p^2_k = 0$, which means that each $\not{p}_k$ and $\bar{\not{p}}_k$ can be decomposed independently into products of Weyl spinors:

$$\not{p}_k = |k]\langle k| \leftrightarrow \tilde{\lambda}^{\dot\alpha}_k \lambda^\beta_k, \quad \bar{\not{p}}_k = |k\rangle[k| \leftrightarrow \lambda_{k,\alpha}\tilde{\lambda}_{k,\dot\beta}. \tag{3.15}$$

As an example of $\not{p} = \sum_k \not{p}_k$ being decomposed between two Weyl spinors $[i|$ and $|j\rangle$, we have
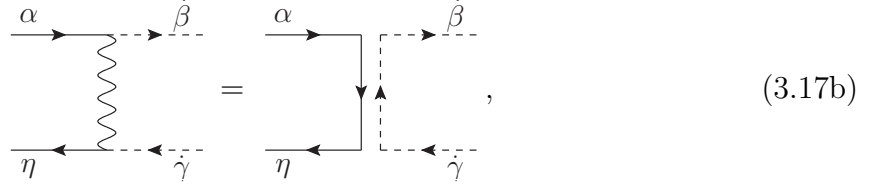
$$[i|\not{p}|j\rangle = [i|\left(\sum_k \not{p}_k\right)|j\rangle = [i|\left(\sum_k |k]\langle k|\right)|j\rangle = \sum_k [ik]\langle kj\rangle, \tag{3.16}$$

forming a sum of Weyl spinor contractions.

The vector boson propagator in Feynman gauge is simply proportional to the metric tensor $g^{\mu\nu}$. The relation between $g^{\mu\nu}$ and the τ matrices in eq. (2.6), together with the Fierz identity,

$$\bar{\tau}^\mu_{\alpha\dot\beta}\tau^{\dot\gamma\eta}_\mu = \delta_\alpha{}^\eta\delta^{\dot\gamma}{}_{\dot\beta} \tag{3.17a}$$

8

which is diagrammatically,

$$\hspace{3cm} = \hspace{4cm}, \hspace{2cm} (3.17b)$$

means that we can write:

$$\mu \,\sim\!\!\sim\!\!\sim^{p}\!\!\sim\!\!\sim\, \nu \;=\; \frac{-ig^{\mu\nu}}{p^2} \leftrightarrow \frac{-i}{p^2} \;\text{-----------}\;. \hspace{2cm} (3.18)$$

When substituting the vector boson propagator we need to make sure that we use one dotted and one undotted line. It is not important which way a specific flow arrow points, only that they are opposite for the two lines, and for that reason they can be completely left out of the generic diagram above.

In some cases it is possible to have τ-contractions in the form of

$$\tau^{\mu,\dot{\alpha}\beta}\tau_\mu^{\dot{\gamma}\eta} = \epsilon^{\dot{\alpha}\dot{\gamma}}\epsilon^{\beta\eta} \quad \text{or} \quad \bar{\tau}^\mu_{\alpha\dot{\beta}}\bar{\tau}_{\mu,\gamma\dot{\eta}} = \epsilon_{\alpha\gamma}\epsilon_{\dot{\beta}\dot{\eta}}. \hspace{2cm} (3.19)$$

However, it is always possible to flip a τ to a $\bar{\tau}$ or vice versa so that there is exactly one τ and one $\bar{\tau}$ so that the Fierz identity in eq. (3.17a) can be used. The details of this can be found in [1].

The positive and negative helicity states for the polarization vectors can be written

$$\varepsilon_+^{*\mu}(p_i, r) = \frac{\lambda_r^\alpha \bar{\tau}^\mu_{\alpha\dot{\beta}} \tilde{\lambda}_i^{\dot{\beta}}}{\lambda_r^\gamma \lambda_{i,\gamma}} = \frac{\langle r|\bar{\tau}^\mu|i]}{\langle ri\rangle}, \hspace{2cm} (3.20a)$$

$$\varepsilon_-^{*\mu}(p_i, r) = \frac{\lambda_i^\alpha \bar{\tau}^\mu_{\alpha\dot{\beta}} \tilde{\lambda}_r^{\dot{\beta}}}{\tilde{\lambda}_{i,\dot{\gamma}} \tilde{\lambda}_r^{\dot{\gamma}}} = \frac{\langle i|\bar{\tau}^\mu|r]}{[ir]}, \hspace{2cm} (3.20b)$$

and upon contraction with τ_μ we get

$$\varepsilon_+^{*\mu}(p_i, r)\tau_\mu^{\dot{\alpha}\beta} = \varepsilon_+^{*\dot{\alpha}\beta}(p_i, r) = \frac{\tilde{\lambda}_i^{\dot{\alpha}}\lambda_r^\beta}{\lambda_r^\gamma \lambda_{i,\gamma}} \leftrightarrow \frac{|i]\langle r|}{\langle ri\rangle} = \frac{1}{\langle ri\rangle} \; \bigcirc\!\text{---}\!\!\rightarrow\!\text{---}\, {}^i_r \;\;, \hspace{1cm} (3.21a)$$

$$\varepsilon_-^{*\mu}(p_i, r)\tau_\mu^{\dot{\alpha}\beta} = \varepsilon_-^{*\dot{\alpha}\beta}(p_i, r) = \frac{\tilde{\lambda}_r^{\dot{\alpha}}\lambda_i^\beta}{\tilde{\lambda}_{i,\dot{\gamma}} \tilde{\lambda}_r^{\dot{\gamma}}} \leftrightarrow \frac{|r]\langle i|}{[ir]} = \frac{1}{[ir]} \; \bigcirc\!\text{---}\!\!\leftarrow\!\text{---}\, {}^r_i \;\;, \hspace{1cm} (3.21b)$$

where p_i refers to the physical momentum of the particle and r is an arbitrary light-like reference momentum.

It is possible to write the two expressions in eq. (3.21) into a more general form,

$$\varepsilon_h^{*\dot{\alpha}\beta}(p_i, r) = \frac{\tilde{\lambda}_{i_p}^{\dot{\alpha}}\lambda_{i_m}^\beta}{\lambda_{i_m}^\gamma \lambda_{i_p,\gamma}} \leftrightarrow \frac{|i_p]\langle i_m|}{f_h(i_p, i_m)} = \frac{1}{f_h(i_p, i_m)} \; \bigcirc\!\text{---}\!\!\rightarrow\!\text{---}\, {}^{i_p}_{i_m} \;\;, \hspace{1cm} (3.22)$$

9

where for $h = \pm$ we have

$$
\begin{aligned}
h = + : & \quad i_p = i, \ i_m = r, \ f_h(i_p, i_m) = \langle ri \rangle, \\
h = - : & \quad i_p = r, \ i_m = i, \ f_h(i_p, i_m) = [ir].
\end{aligned}
\tag{3.23}
$$

It is possible to choose different reference momenta r_i for different particles i, and the dependence on the reference momenta will vanish for gauge invariant quantities. The choice of reference momenta can be made for convenience, to make certain diagrams vanish. A common choice is to choose the reference momenta of all like-helicity bosons to be equal to the physical momentum of a boson with the opposite helicity, which is useful because we have the relations:

$$
\varepsilon_\pm^*(p_1, r) \cdot \varepsilon_\pm^*(p_2, r) = 0 \quad \text{and} \quad \varepsilon_\pm^*(p_1, p_2) \cdot \varepsilon_\mp^*(p_2, r_2) = 0.
\tag{3.24}
$$

The triple and quartic gluon vertices can be written as

$$
= -\frac{g_s f^{a_1 a_2 a_3}}{\sqrt{2}} \left[g^{\mu_1 \mu_2} (p_1 - p_2)^{\mu_3} + g^{\mu_2 \mu_3} (p_2 - p_3)^{\mu_1} + g^{\mu_3 \mu_1} (p_3 - p_1)^{\mu_2} \right]
$$

$$
\leftrightarrow -\frac{g_s f^{a_1 a_2 a_3}}{2} \left[\vcenter{\hbox{}} + \vcenter{\hbox{}} + \vcenter{\hbox{}} \right],
\tag{3.25}
$$

$$
= -i g_s^2 [f^{a_1 a_2 b} f^{a_4 a_3 b} (g^{\mu_1 \mu_4} g^{\mu_2 \mu_3} - g^{\mu_1 \mu_3} g^{\mu_2 \mu_4})
$$

$$
+ f^{a_1 a_4 b} f^{a_2 a_3 b} (g^{\mu_1 \mu_2} g^{\mu_3 \mu_4} - g^{\mu_1 \mu_3} g^{\mu_2 \mu_4})
$$

$$
+ f^{a_1 a_3 b} f^{a_2 a_4 b} (g^{\mu_1 \mu_2} g^{\mu_3 \mu_4} - g^{\mu_1 \mu_4} g^{\mu_2 \mu_3})]
$$

$$
= i \left(\frac{g_s}{\sqrt{2}} \right)^2 \sum_{S(2,3,4)} \text{Tr}(t^{a_1} t^{a_2} t^{a_3} t^{a_4}) \left[2 g^{\mu_1 \mu_3} g^{\mu_4 \mu_2} - g^{\mu_1 \mu_2} g^{\mu_3 \mu_4} - g^{\mu_1 \mu_4} g^{\mu_2 \mu_3} \right]
\tag{3.26}
$$

$$
\leftrightarrow i \left(\frac{g_s}{\sqrt{2}} \right)^2 \sum_{S(2,3,4)} \text{Tr}(t^{a_1} t^{a_2} t^{a_3} t^{a_4}) \left[2 \vcenter{\hbox{}} - \vcenter{\hbox{}} - \vcenter{\hbox{}} \right].
\tag{3.27}
$$

The $g^{\mu_i \mu_j}$ factors become double lines via the Fierz identity and the p^μ factors are replaced using eq. (3.10).

3.2 Diagram Examples

Now that the basics of the chirality-flow method for massless QED and QCD tree-level diagrams have been presented, let us look at some examples. In these examples all particles are considered outgoing. There are also often multiple diagrams contributing to a specific process, but here we are looking purely at individual diagrams. Something to keep in mind is that in the massless case only one chirality contributes to a certain helicity. This means that in the first example below, the two fermions that share a fermion line need to have opposite helicities for a non-zero amplitude; chirality flips at the vertex, and therefore helicity must do the same.

We start with the simplest example, which just consists of four fermion legs and a photon propagator, which can be used to calculate amplitudes for processes such as $e^- e^+ \to \mu^- \mu^+$. In this diagram the $+$ and $-$ labels refer to the helicity of the particle. We collect all the
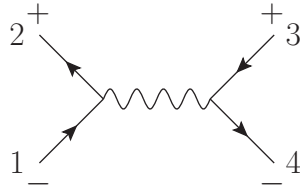
Figure 1: A four-fermion diagram with a given helicity configuration.

necessary factors from the vertices and the photon propagator together, and apply the rules given in eq. (3.5) to transform the Feynman diagram into a chirality-flow diagram. The positive helicity (left-chiral) particles are replaced with dotted lines, the negative helicity (right-chiral) particles are replaced with undotted lines, and the photon propagator is replaced with a double line whose arrow directions are fitted to the arrow directions of the external legs. The result is:

$$= \frac{2ie^2}{(p_1 + p_2)^2}$$

$$= \frac{2ie^2 \, [23] \, \langle 41 \rangle}{(p_1 + p_2)^2},$$

where in the final step, the two lines have been written as their spinor contractions. Note that the final step is completely trivial; the chirality-flow lines *are* the spinor contractions. Another type of diagram we can look at is one with a fermion propagator instead of a photon propagator. One example is a diagram with two fermion legs and two photon legs: Again we have a Feynman diagram with a specific helicity configuration. The helicities of the external photons do not actually have to be specified at this stage as they can be given in the generic form of eq. (3.22), but have been anyway for demonstrative purposes. In this example we have two new objects that were not seen in the first example: the fermion propagator and the external photon or vector boson in general. By again collecting the
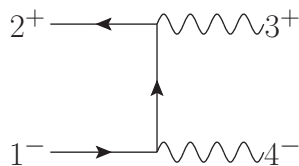
11

Figure 2: A $f f \gamma \gamma$ diagram with a given helicity configuration. The fermions are considered massless.

relevant factors, and in this example also including the two factors in the denominator from the photon polarization vectors, we get:

$$
\text{} = \frac{-2ie^2}{(p_2 + p_3)^2 \langle r_3 3 \rangle [4 r_4]} \text{} \tag{3.28a}
$$

$$
= \frac{-2ie^2}{(p_2 + p_3)^2 \langle r_3 3 \rangle [4 r_4]} [23] \Big(\langle r_3 2 \rangle [2 r_4] + \langle r_3 3 \rangle [3 r_4] \Big) \langle 41 \rangle, \tag{3.28b}
$$

where r_3 and r_4 are the light-like reference momenta of the two photons. We have used eq. (3.21) for the external photons here. Since all particles are considered outgoing, the momentum flowing through the fermion propagator can be written as either $p_2 + p_3$ or $-(p_1 + p_4)$. Since all four particles are massless, we can use eq. (3.16) for the propagator line. As an example, we can here make a clever choice of reference momentum $r_4 = p_2$ which simplifies this expression to

$$
\text{} = \frac{2ie^2 [23]^2 \langle 41 \rangle}{(p_2 + p_3)^2 [42]} \tag{3.29}
$$

Before continuing, take an extra moment to admire the simplicity of the method used in the examples above. It is possible by using the chirality-flow method to go from a Feynman diagram to a complex number in a line or two of calculation, practically instantly after some practice.

4 Massive Particles

We would like to extend the chirality-flow method to include massive particles. Spinor-helicity methods and the Weyl-van-der-Waerden formalism are known for massive particles [9], and this reference will be used extensively throughout this entire section. In this section we discuss massive spinors, bispinors, and polarization vectors, to express them in a form which will be used to include them in the chirality-flow method in section 5. We will start with bispinors.

12

4.1 Bispinor Decomposition

We would like to decompose $\not{p}$ and $\bar{\not{p}}$ into products of Weyl spinors. If their determinants are zero, as they are in the massless case where p^μ is light-like, then it is possible to decompose them both directly,

$$\not{p} = |p]\langle p|, \quad \bar{\not{p}} = |p\rangle[p|, \tag{4.1a}$$

or in index form as

$$\sqrt{2}p^{\dot{\alpha}\beta} = \tilde{p}^{\dot{\alpha}}p^\beta, \quad \sqrt{2}\bar{p}_{\alpha\dot{\beta}} = p_\alpha\tilde{p}_{\dot{\beta}}, \tag{4.1b}$$

where we now use p directly instead of λ_p as $\lambda_\pm$ will in the remaining part of the thesis be used for the two eigenvalues of $\not{p}$ and $\bar{\not{p}}$. If $\det(\not{p}) = \det(\bar{\not{p}}) = p^2 = m^2 \neq 0$, then we need to split p into a sum of two terms that are decomposed separately. We may decompose using the eigenvalues of $\not{p}$ and $\bar{\not{p}}$, or use a more general light-like decomposition. The eigenvalue decomposition is a special case of the more general type of decomposition, and it is more symmetric and intuitive. The general light-like decomposition, however, gives us freedom to choose a particular decomposition, which can be used to cancel certain parts of our calculations.

4.1.1 Eigenvalue Decomposition

The eigenvalue decomposition involves the eigenvalues and eigenvectors of $\not{p}$ and $\bar{\not{p}}$. The eigenvalues can be found through the characteristic equation, $\det(\not{p} - \lambda\mathbb{1}) = 0$, and they are, for both $\not{p}$ and $\bar{\not{p}}$,

$$\lambda_\pm = p^0 \pm |\mathbf{p}|. \tag{4.2}$$

Note that in the massless limit, where $p^2 = (p^0)^2 - |\mathbf{p}|^2 = 0$, we get $\lambda_+ = 2p^0 = 2|\mathbf{p}|$ and $\lambda_- = 0$. We also have the relation

$$\det(\not{p}) = \det(\bar{\not{p}}) = \lambda_+\lambda_- = p^2 = m^2. \tag{4.3}$$

We wish to find the eigenvectors $|n_\pm]$ and $|n_\pm\rangle$ so that

$$\not{p} = \lambda_+|n_+]\langle n_+| + \lambda_-|n_-]\langle n_-| \quad \text{and} \quad \bar{\not{p}} = \lambda_+|n_+\rangle[n_+| + \lambda_-|n_-\rangle[n_-|. \tag{4.4}$$

These eigenvectors for the two matrices can be found in the standard way using matrix multiplication:

$$\tilde{n}_+^{\dot{\alpha}} \leftrightarrow |n_+] = e^{-i\rho}\begin{pmatrix} \sin\frac{\theta}{2} \\ -e^{i\phi}\cos\frac{\theta}{2} \end{pmatrix}, \quad \tilde{n}_-^{\dot{\alpha}} \leftrightarrow |n_-] = e^{i\rho}\begin{pmatrix} -e^{-i\phi}\cos\frac{\theta}{2} \\ -\sin\frac{\theta}{2} \end{pmatrix}, \tag{4.5a}$$

$$n_{+,\alpha} \leftrightarrow |n_+\rangle = e^{i\rho}\begin{pmatrix} e^{-i\phi}\cos\frac{\theta}{2} \\ \sin\frac{\theta}{2} \end{pmatrix}, \quad n_{-,\alpha} \leftrightarrow |n_-\rangle = e^{-i\rho}\begin{pmatrix} \sin\frac{\theta}{2} \\ -e^{i\phi}\cos\frac{\theta}{2} \end{pmatrix}, \tag{4.5b}$$

13

where ρ is an arbitrary phase and where we have used spherical polar coordinates,

$$\mathbf{p} = |\mathbf{p}|\,\mathbf{e}, \quad \mathbf{e} = \begin{pmatrix} \cos\phi\sin\theta \\ \sin\phi\sin\theta \\ \cos\theta \end{pmatrix}. \tag{4.6}$$

The eigenvectors are normalized to satisfy $1 = \langle n_+ n_- \rangle = [n_- n_+]$, which is later used to normalize the Dirac spinors in eq. (4.31). We note that from eq. (4.5) we get the relations

$$|n_+] = |n_-\rangle \quad \text{and} \quad |n_-] = -|n_+\rangle. \tag{4.7}$$

There is a possible source of confusion regarding the eigenvalue equation due to the spinor contractions being antisymmetric. What we get when applying $\not{p}$ to $|n_+\rangle$ is

$$\not{p}|n_+\rangle = \Big(\lambda_+|n_+]\langle n_+| + \lambda_-|n_-]\langle n_-|\Big)|n_+\rangle = \lambda_-|n_-]\,\langle n_- n_+\rangle = -\lambda_-|n_-], \tag{4.8}$$

which does not look like an eigenvalue equation. However, since $|n_-] = -|n_+\rangle$ we can rewrite this equation into the form of an eigenvalue equation,

$$\not{p}|n_-] = \lambda_-|n_-]. \tag{4.9a}$$

The same method can be used to write out the other 3 eigenvalue equations:

$$\not{p}|n_+] = \lambda_+|n_+], \tag{4.9b}$$

$$\bar{\not{p}}|n_-\rangle = \lambda_-|n_-\rangle, \tag{4.9c}$$

$$\bar{\not{p}}|n_+\rangle = \lambda_+|n_+\rangle. \tag{4.9d}$$

The conclusion of this discussion is that the eigenvectors for $\not{p}$ are $|n_\pm]$ and the eigenvectors for $\bar{\not{p}}$ are $|n_\pm\rangle$.

We can rewrite the decompositions in eq. (4.4) by letting the two Weyl spinors each absorb a factor of $\sqrt{\lambda}$,

$$|p_\pm] = \sqrt{\lambda_\pm}|n_\pm], \quad |p_\pm\rangle = \sqrt{\lambda_\pm}|n_\pm\rangle, \tag{4.10}$$

so that $\not{p}$ and $\bar{\not{p}}$ can be written as

$$\not{p} = |p_+]\langle p_+| + |p_-]\langle p_-| \quad \text{and} \quad \bar{\not{p}} = |p_+\rangle[p_+| + |p_-\rangle[p_-|. \tag{4.11}$$

In this new form, $\langle p_+ p_- \rangle = \sqrt{\lambda_+\lambda_-} = m$ and eq. (4.7) turns into

$$\sqrt{\lambda_-}|p_+] = \sqrt{\lambda_+}|p_-\rangle \quad \text{and} \quad \sqrt{\lambda_+}|p_-] = -\sqrt{\lambda_-}|p_+\rangle. \tag{4.12}$$

We also list these relations:

$$\not{p}|p_+\rangle = |p_-]\,\langle p_- p_+\rangle = -m|p_-], \tag{4.13a}$$

$$\not{p}|p_-\rangle = |p_+]\,\langle p_+ p_-\rangle = m|p_+], \tag{4.13b}$$

$$\bar{\not{p}}|p_+] = |p_-\rangle\,[p_- p_+] = m|p_-\rangle, \tag{4.13c}$$

$$\bar{\not{p}}|p_-] = |p_+\rangle\,[p_+ p_-] = -m|p_+\rangle, \tag{4.13d}$$

which will be used to find the Dirac equation solutions in eq. (4.30).

4.1.2 General Light-like Decomposition

A more general way to decompose p^μ is to write it as

$$p^\mu = p^{\flat\mu} + \alpha q^\mu, \quad \alpha = \frac{p^2}{2p\cdot q}, \quad p\cdot q \neq 0. \tag{4.14}$$

Note that $p\cdot q = (p^\flat + \alpha q)\cdot q = p^\flat \cdot q$ since $q^2 = 0$. We may choose a light-like four-vector q^μ arbitrarily, which determines the other light-like four-vector $p^{\flat\mu}$. It is straightforward to verify that $p^{\flat\mu}$ is indeed light-like:

$$(p^\flat)^2 = p^2 - 2\frac{p^2}{2p\cdot q}p\cdot q + \alpha^2 q^2 = \alpha^2 q^2 = 0, \tag{4.15}$$

since $q^2 = 0$.

We have found two light-like four-vectors $p^{\flat\mu}$ and q^μ which means that we can now write $\not{p}$ and $\bar{\not{p}}$ as

$$\not{p} = |p^\flat]\langle p^\flat| + \alpha|q]\langle q| \quad \text{and} \quad \bar{\not{p}} = |p^\flat\rangle[p^\flat| + \alpha|q\rangle[q|, \tag{4.16a}$$

or in index form as

$$\sqrt{2}p^{\dot\alpha\beta} = \tilde{p}^{\flat\dot\alpha}p^{\flat\beta} + \alpha\tilde{q}^{\dot\alpha}q^\beta \quad \text{and} \quad \sqrt{2}\bar{p}_{\alpha\dot\beta} = p^\flat_\alpha\tilde{p}^\flat_{\dot\beta} + \alpha q_\alpha\tilde{q}_{\dot\beta}. \tag{4.16b}$$

Explicit expressions for the $p^\flat$ and q Weyl spinors can be found using eq. (3.6). In the massless limit, $\alpha = \frac{p^2}{2p\cdot q} = \frac{m^2}{2p\cdot q} = 0$, which means that $p^{\flat\mu} \to p^\mu$ so eq. (4.16) trivially reduces to eq. (4.1).

The specific choice of q^μ that gives the eigenvalue decomposition is $q^\mu = \frac{1}{2}(1, -\mathbf{e})$, which is clearly light-like since $\mathbf{e}$ is the unit vector in spherical polar coordinates given in eq. (4.6). With $(p^0, |\mathbf{p}|\,\mathbf{e}) = p^\mu = p^{\flat\mu} + \alpha q^\mu$ we find that

$$2p\cdot q = p^0\cdot 1 + |\mathbf{p}|\,\mathbf{e}\cdot\mathbf{e} = p^0 + |\mathbf{p}| = \lambda_+, \tag{4.17}$$

$$\alpha = \frac{p^2}{2p\cdot q} = \frac{\lambda_+\lambda_-}{\lambda_+} = \lambda_-, \tag{4.18}$$

$$p^{\flat\mu} = p^\mu - \alpha q^\mu = (p^0, |\mathbf{p}|\,\mathbf{e}) - \frac{\lambda_-}{2}(1, -\mathbf{e}) = \frac{\lambda_+}{2}(1, \mathbf{e}). \tag{4.19}$$

The decomposition of p^μ can in this case be written as

$$p^\mu = \lambda_+ n^\mu_+ + \lambda_- n^\mu_-, \quad \text{where} \quad n^\mu_+ = \frac{1}{2}(1, \mathbf{e}) \quad \text{and} \quad n^\mu_- = \frac{1}{2}(1, -\mathbf{e}), \tag{4.20}$$

where p^μ has been split into light-like forward-pointing and backward-pointing components. We can also define:

$$p^\mu_\pm = \lambda_\pm n^\mu_\pm \tag{4.21}$$

15

The backward-pointing component will vanish in the massless case as λ_- goes to zero. Contracting this p^μ with either σ^μ or $\bar{\sigma}^\mu$ gives us back the two expressions in eq. (4.4), or to express it another way:

$$|n_+]\langle n_+| = n_+^\mu \sigma_\mu, \quad |n_-]\langle n_-| = n_-^\mu \sigma_\mu, \tag{4.22a}$$

$$|n_+\rangle[n_+| = n_+^\mu \bar{\sigma}_\mu, \quad |n_-\rangle[n_-| = n_-^\mu \bar{\sigma}_\mu, \tag{4.22b}$$

which is straightforward but tedious to verify component-wise.

We would like to find expressions for the different types of spinor contractions between $p^\flat$ and q. Due to their antisymmetry and the relation $\left[p^\flat q\right]^* = \left\langle qp^\flat \right\rangle$ we only need to find one of them, because the others can be easily found using these relations. We have for any 4-vectors p and k the relation

$$\bar{p}_{\alpha\dot{\beta}}k^{\dot{\beta}\alpha} = p^\mu \bar{\tau}_{\mu,\alpha\dot{\beta}}k^\nu \tau_\nu^{\dot{\beta}\alpha} = p^\mu k^\nu g_{\mu\nu} = p \cdot k, \tag{4.23}$$

where we have used eq. (2.6). We can use the relation above to rewrite the product of p^μ and q^μ in terms of Weyl spinors,

$$2p \cdot q = \sqrt{2}\bar{p}_{\alpha\dot{\beta}}\sqrt{2}q^{\dot{\beta}\alpha} = \sqrt{2}\bar{p}_{\alpha\dot{\beta}}\tilde{q}^{\dot{\beta}}q^\alpha = (p_\alpha^\flat \tilde{p}_{\dot{\beta}}^\flat + \alpha q_\alpha \tilde{q}_{\dot{\beta}})\tilde{q}^{\dot{\beta}}q^\alpha = q^\alpha p_\alpha^\flat \tilde{p}_{\dot{\beta}}^\flat \tilde{q}^{\dot{\beta}}$$
$$= \left\langle qp^\flat \right\rangle \left[p^\flat q\right] = \left|\left[p^\flat q\right]\right|^2, \tag{4.24}$$

which gives us one of the expressions we seek,

$$\left[p^\flat q\right] = e^{i\varphi}\sqrt{2p \cdot q} = e^{i\varphi}\frac{m}{\sqrt{\alpha}}, \tag{4.25a}$$

where $2p \cdot q > 0$ and φ is an arbitrary phase. From this we get the three others,

$$\left[qp^\flat\right] = -e^{i\varphi}\sqrt{2p \cdot q} = -e^{i\varphi}\frac{m}{\sqrt{\alpha}}, \tag{4.25b}$$

$$\left\langle qp^\flat\right\rangle = e^{-i\varphi}\sqrt{2p \cdot q} = e^{-i\varphi}\frac{m}{\sqrt{\alpha}}, \tag{4.25c}$$

$$\left\langle p^\flat q\right\rangle = -e^{-i\varphi}\sqrt{2p \cdot q} = -e^{-i\varphi}\frac{m}{\sqrt{\alpha}}. \tag{4.25d}$$

It is possible to express the $p^\flat$ Weyl spinors entirely in terms of p and q, which will be used in eq. (4.41). The equation

$$\bar{\slashed{p}}|q] = \left(|p^\flat\rangle[p^\flat| + \alpha|q\rangle[q|\right)|q] = |p^\flat\rangle\left[p^\flat q\right] = |p^\flat\rangle e^{i\varphi}\sqrt{2p \cdot q} \tag{4.26}$$

can be used to fit this purpose. We do a similar calculation for $\slashed{p}|q\rangle$, rearrange the two equations, and arrive at:

$$|p^\flat] = \frac{-e^{i\varphi}}{\sqrt{2p \cdot q}}\slashed{p}|q\rangle, \quad |p^\flat\rangle = \frac{e^{-i\varphi}}{\sqrt{2p \cdot q}}\bar{\slashed{p}}|q]. \tag{4.27}$$

4.2 Dirac Equation Solutions

The solutions to the Dirac equation $(i\partial\!\!\!/_\gamma - m)\Psi = 0$, with Ψ being the Dirac spinor in position space, can be divided into positive and negative frequency solutions,

$$\Psi^+ = e^{-ip\cdot x}u^s(p) = e^{-ip\cdot x}\begin{pmatrix} |u_L^s] \\ |u_R^s\rangle \end{pmatrix}, \quad \Psi^- = e^{ip\cdot x}v^s(p) = e^{ip\cdot x}\begin{pmatrix} |v_L^s] \\ |v_R^s\rangle \end{pmatrix}, \tag{4.28}$$

where s is the spin index and where the particle spinor $u^s(p)$ and anti-particle spinor $v^s(p)$ have been split into their left- and right-chiral parts. Since we are using the chiral basis, we can separate the Dirac equation into two parts in both cases:

$$p\!\!\!/|u_R^s\rangle = m|u_L^s] \quad \text{and} \quad \bar{p}\!\!\!/|u_L^s] = m|u_R^s\rangle \tag{4.29a}$$

or

$$p\!\!\!/|v_R^s\rangle = -m|v_L^s] \quad \text{and} \quad \bar{p}\!\!\!/|v_L^s] = -m|v_R^s\rangle. \tag{4.29b}$$

4.2.1 In The Eigenvalue Decomposition

Using the eigenvalue decomposition in eq. (4.11) for $p\!\!\!/$ and $\bar{p}\!\!\!/$ we can write the solutions as

$$u^+(p) = \begin{pmatrix} -|p_-] \\ |p_+\rangle \end{pmatrix}, \quad u^-(p) = \begin{pmatrix} |p_+] \\ |p_-\rangle \end{pmatrix},$$

$$v^+(p) = \begin{pmatrix} |p_+] \\ -|p_-\rangle \end{pmatrix}, \quad v^-(p) = \begin{pmatrix} |p_-] \\ |p_+\rangle \end{pmatrix}, \tag{4.30}$$

which can be verified by using eq. (4.13). Here the labels for the Dirac spinors refer to the helicities of the particles and the Weyl spinor labels refer to the eigenvalues $\lambda_\pm$ used in the eigenvalue decomposition. These solutions are normalized as:

$$u^{s\dagger}(p)u^r(p) = v^{s\dagger}(p)v^r(p) = 2p^0\delta^{sr}, \ \bar{u}^s(p)u^r(p) = 2m\delta^{sr}, \text{ and } \bar{v}^s(p)v^r(p) = -2m\delta^{sr}. \tag{4.31}$$

To show that the spin labels in eq. (4.30) actually refer to the helicities we use the helicity projector $\Sigma^\pm = \frac{1}{2}\left(1 \pm \gamma^5 s\!\!\!/_\gamma\right)$, where $s^\mu = \frac{p^0}{m|\mathbf{p}|}p^\mu - g^{\mu 0}\frac{m}{|\mathbf{p}|}$ is the spin vector, which satisfies $s^2 = -1$ and $s \cdot p = 0$ [10, 11]. The spin vector can also be written as $s^\mu = \frac{1}{m}(p_+^\mu - p_-^\mu)$, where p_+^μ and p_-^μ are given in eq. (4.21). The helicity projector together with the Dirac equation solutions satisfy:

$$\Sigma^+u^+ = u^+, \quad \Sigma^-u^+ = 0, \tag{4.32a}$$
$$\Sigma^-u^- = u^-, \quad \Sigma^+u^- = 0, \tag{4.32b}$$
$$\Sigma^+v^+ = v^+, \quad \Sigma^-v^+ = 0, \tag{4.32c}$$
$$\Sigma^-v^- = v^-, \quad \Sigma^+v^- = 0. \tag{4.32d}$$

These can all be verified in the same way. For the u^+ spinor we have

$$\gamma^5 \slashed{p}_\gamma u^+ = \begin{pmatrix} 0 & \frac{1}{m}\left(\slashed{p}_- - \slashed{p}_+\right) \\ \frac{1}{m}\left(\bar{\slashed{p}}_+ - \bar{\slashed{p}}_-\right) & 0 \end{pmatrix} \begin{pmatrix} -|p_-] \\ |p_+\rangle \end{pmatrix} = \begin{pmatrix} \frac{1}{m}\slashed{p}_-|p_+\rangle \\ -\frac{1}{m}\bar{\slashed{p}}_+|p_-] \end{pmatrix}$$

$$= \begin{pmatrix} \frac{1}{m}|p_-]\langle p_- p_+\rangle \\ -\frac{1}{m}|p_+\rangle [p_+ p_-] \end{pmatrix} = \begin{pmatrix} \frac{1}{m}|p_-](-m) \\ -\frac{1}{m}|p_+\rangle(-m) \end{pmatrix} = \begin{pmatrix} -|p_-] \\ |p_+\rangle \end{pmatrix} = u^+, \qquad (4.33)$$

where we use $\slashed{p}_+|p_+\rangle = |p_+] \langle p_+ p_+\rangle = 0$, $\bar{\slashed{p}}_-|p_-] = |p_-\rangle [p_- p_-] = 0$, and eq. (4.13). This gives us for the helicity projectors:

$$\begin{cases} \Sigma^+ u^+ = \frac{1}{2}\left(1 + \gamma^5 \slashed{p}_\gamma\right)u^+ = \frac{1}{2}(1+1)\,u^+ = u^+ \\ \Sigma^- u^+ = \frac{1}{2}\left(1 - \gamma^5 \slashed{p}_\gamma\right)u^+ = \frac{1}{2}(1-1)\,u^+ = 0 \end{cases}. \qquad (4.34)$$

To find the outgoing particle spinors from the solutions we have, we simply need to Dirac conjugate the u-spinors. In total we then have

$$\bar{u}^+ = \left([p_+| \quad -\langle p_-|\right) \qquad \leftrightarrow \quad \text{outgoing } (+) \text{ helicity fermion,} \qquad (4.35a)$$

$$\bar{u}^- = \left([p_-| \quad \langle p_+|\right) \qquad \leftrightarrow \quad \text{outgoing } (-) \text{ helicity fermion,} \qquad (4.35b)$$

$$v^+ = \begin{pmatrix} |p_+] \\ -|p_-\rangle \end{pmatrix} \qquad \leftrightarrow \quad \text{outgoing } (+) \text{ helicity anti-fermion,} \qquad (4.35c)$$

$$v^- = \begin{pmatrix} |p_-] \\ |p_+\rangle \end{pmatrix} \qquad \leftrightarrow \quad \text{outgoing } (-) \text{ helicity anti-fermion.} \qquad (4.35d)$$

4.2.2   In The General Light-like Decomposition

If instead the $\slashed{p}$ and $\bar{\slashed{p}}$ in the Dirac equation are decomposed in the general light-like decomposition, the solutions can be written as

$$u^+ = \begin{pmatrix} -\sqrt{\alpha}|q] \\ -e^{i\varphi}|p^b\rangle \end{pmatrix}, \quad u^- = \begin{pmatrix} -e^{-i\varphi}|p^b] \\ \sqrt{\alpha}|q\rangle \end{pmatrix}, \qquad (4.36)$$

$$v^+ = \begin{pmatrix} -e^{-i\varphi}|p^b] \\ -\sqrt{\alpha}|q\rangle \end{pmatrix}, \quad v^- = \begin{pmatrix} \sqrt{\alpha}|q] \\ -e^{i\varphi}|p^b\rangle \end{pmatrix}, \qquad (4.37)$$

and the outgoing particle spinors as

$$\bar{u}^+ = \left(-e^{-i\varphi}[p^b| \quad -\sqrt{\alpha}\langle q|\right) \quad \leftrightarrow \text{outgoing } (+) \text{ spin fermion} \qquad (4.38a)$$

$$\bar{u}^- = \left(\sqrt{\alpha}[q| \quad -e^{i\varphi}\langle p^b|\right) \quad \leftrightarrow \text{outgoing } (-) \text{ spin fermion} \qquad (4.38b)$$

$$v^+ = \begin{pmatrix} -e^{-i\varphi}|p^b] \\ -\sqrt{\alpha}|q\rangle \end{pmatrix} \qquad\qquad \leftrightarrow \text{outgoing } (+) \text{ spin anti-fermion} \qquad (4.38c)$$

$$v^- = \begin{pmatrix} \sqrt{\alpha}|q] \\ -e^{i\varphi}|p^b\rangle \end{pmatrix} \qquad\qquad \leftrightarrow \text{outgoing } (-) \text{ spin anti-fermion,} \qquad (4.38d)$$

18

where the spin labels do not refer to the helicities in this case, but rather to the spin along an axis defined by the choice of q^μ, namely the spatial part of the spin vector $s^\mu = \frac{p^\mu}{m} - \frac{m}{p \cdot q} q^\mu = \frac{1}{m}\left(p^{\flat\mu} - \alpha q^\mu\right)$. The relations in eq. (4.32) also apply in the general light-like decomposition case, but now we use this spin vector s^μ in $\Sigma^\pm = \frac{1}{2}(1 \pm \gamma^5 \slashed{s}_\gamma)$. It is worth noting that if $q^\mu = \frac{1}{2}(1, -\mathbf{e})$, which is the specific choice of q^μ that turns the general decomposition into the eigenvalue decomposition, then $p^{\flat\mu} = p^\mu_+$, $\alpha q^\mu = p^\mu_-$, and $s^\mu = \frac{1}{m}\left(p^{\flat\mu} - \alpha q^\mu\right) = \frac{1}{m}\left(p^\mu_+ - p^\mu_-\right)$, as it is for the helicity projector used in eq. (4.32).

The relations in eq. (4.32) are verified in the same way for $s^\mu = \frac{1}{m}\left(p^{\flat\mu} - \alpha q^\mu\right)$ as we have done before when $s^\mu = \frac{1}{m}\left(p^\mu_+ - p^\mu_-\right)$. For the u^+ spinor we have

$$\gamma^5 \slashed{s}_\gamma u^+ = \begin{pmatrix} 0 & \frac{1}{m}(\alpha \slashed{q} - \slashed{p}^\flat) \\ \frac{1}{m}(\bar{\slashed{p}}^\flat - \alpha \bar{\slashed{q}}) & 0 \end{pmatrix} \begin{pmatrix} -\sqrt{\alpha}|q] \\ -e^{i\varphi}|p^\flat\rangle \end{pmatrix} = \begin{pmatrix} -\frac{e^{i\varphi}\alpha}{m}\slashed{q}|p^\flat\rangle \\ -\frac{\sqrt{\alpha}}{m}\bar{\slashed{p}}^\flat|q] \end{pmatrix}$$

$$= \begin{pmatrix} -\frac{e^{i\varphi}\alpha}{m}|q]\langle qp^\flat\rangle \\ -\frac{\sqrt{\alpha}}{m}|p^\flat\rangle[p^\flat q] \end{pmatrix} = \begin{pmatrix} -\frac{e^{i\varphi}\alpha}{m}|q](e^{-i\varphi}\frac{m}{\sqrt{\alpha}}) \\ -\frac{\sqrt{\alpha}}{m}|p^\flat\rangle(e^{i\varphi}\frac{m}{\sqrt{\alpha}}) \end{pmatrix} = \begin{pmatrix} -\sqrt{\alpha}|q] \\ -e^{i\varphi}|p^\flat\rangle \end{pmatrix} = u^+, \qquad (4.39)$$

where we have used $\slashed{p}^\flat|p^\flat\rangle = |p^\flat]\langle p^\flat p^\flat\rangle = 0$, $\bar{\slashed{q}}|q] = |q\rangle[qq] = 0$, and eq. (4.25). This gives for the spin projectors $\Sigma^\pm = \frac{1}{2}(1 \pm \gamma^5 \slashed{s}_\gamma)$:

$$\Sigma^+ u^+ = u^+, \quad \Sigma^- u^+ = 0, \qquad (4.40)$$

and similarly for the other combinations of projectors and spinors.

It is possible to write the spinors in a different form, shown here for u^+:

$$u^+ = \begin{pmatrix} -\sqrt{\alpha}|q] \\ -e^{i\varphi}|p^\flat\rangle \end{pmatrix} = \begin{pmatrix} -\frac{m}{\sqrt{2p \cdot q}}|q] \\ -e^{i\varphi}\frac{\slashed{p}|q]}{e^{i\varphi}\sqrt{2p \cdot q}} \end{pmatrix} = -\frac{1}{\sqrt{2p \cdot q}}\begin{pmatrix} m|q] \\ \bar{\slashed{p}}|q] \end{pmatrix}$$

$$= -\frac{1}{\sqrt{2p \cdot q}}(\slashed{p}_\gamma + m)\begin{pmatrix} |q] \\ 0 \end{pmatrix} = \frac{-e^{i\varphi}}{[p^\flat q]}(\slashed{p}_\gamma + m)|q]_D, \qquad (4.41)$$

where we have used eq. (4.25) and eq. (4.27), and where we have introduced an extension of two-component Weyl spinors to four-component Dirac spinors:

$$|q]_D = \begin{pmatrix} |q] \\ 0 \end{pmatrix}, \quad |q\rangle_D = \begin{pmatrix} 0 \\ |q\rangle \end{pmatrix}, \quad [q|_D = \begin{pmatrix} [q| & 0 \end{pmatrix}, \quad \langle q|_D = \begin{pmatrix} 0 & \langle q| \end{pmatrix}. \qquad (4.42)$$

For all four cases we have:

$$\bar{u}^+ = \begin{pmatrix} -e^{-i\varphi}[p^\flat| & -\sqrt{\alpha}\langle q| \end{pmatrix} = \frac{-e^{-i\varphi}}{\langle qp^\flat\rangle}\langle q|_D(\slashed{p}_\gamma + m), \qquad (4.43a)$$

$$\bar{u}^- = \begin{pmatrix} \sqrt{\alpha}[q| & -e^{i\varphi}\langle p^\flat| \end{pmatrix} = \frac{-e^{i\varphi}}{[qp^\flat]}[q|_D(\slashed{p}_\gamma + m), \qquad (4.43b)$$

$$v^+ = \begin{pmatrix} -e^{-i\varphi}|p^\flat] \\ -\sqrt{\alpha}|q\rangle \end{pmatrix} = \frac{-e^{-i\varphi}}{\langle p^\flat q\rangle}(\slashed{p}_\gamma - m)|q\rangle_D, \qquad (4.43c)$$

$$v^- = \begin{pmatrix} \sqrt{\alpha}|q] \\ -e^{i\varphi}|p^\flat\rangle \end{pmatrix} = \frac{-e^{i\varphi}}{[p^\flat q]}(\slashed{p}_\gamma - m)|q]_D. \qquad (4.43d)$$

4.3 Polarization Vectors

All polarization vectors ε^μ should satisfy the transversality condition,

$$p^\mu \varepsilon_\mu(p) = 0, \tag{4.44}$$

and the orthonormality relation,

$$\varepsilon_i^\mu(p)\varepsilon_{j,\mu}^*(p) = -\delta_{ij}. \tag{4.45}$$

for $i, j = +, 0, -$ being the three polarisation states for massive particles.

4.3.1 In The Eigenvalue Decomposition

In the helicity basis, which we have seen in the previous section is related to the eigenvalue decomposition, the three polarization states can be expressed as:

$$\varepsilon_\pm^\mu(p) = \frac{e^{\mp i\phi}}{\sqrt{2}}\left(0, -\cos\theta\cos\phi \pm i\sin\phi, -\cos\theta\sin\phi \mp i\cos\phi, \sin\theta\right) = \varepsilon_\mp^{*\mu}(p), \tag{4.46a}$$

$$\varepsilon_0^\mu(p) = \frac{p^0}{m}\left(\frac{|\mathbf{p}|}{p^0}, \cos\phi\sin\theta, \sin\phi\sin\theta, \cos\theta\right) = \frac{1}{m}(p_+^\mu - p_-^\mu) = s^\mu, \tag{4.46b}$$

where we have used the spherical polar coordinates defined in eq. (4.6). We consider outgoing particles and therefore the complex conjugated polarization vectors. The matrix or bispinor form can be found by contracting $\varepsilon_i^{*\mu}(p)$ with either $\tau^{\mu,\dot\alpha\beta}$ or $\bar\tau_{\alpha\dot\beta}^\mu$, and they are:

$$\varepsilon_+^{*\dot\alpha\beta}(p) \leftrightarrow e^{2i\rho}|n_+]\langle n_-|, \qquad\qquad \bar\varepsilon_{+,\alpha\dot\beta}^*(p) \leftrightarrow e^{2i\rho}|n_-\rangle[n_+|, \tag{4.47a}$$

$$\varepsilon_-^{*\dot\alpha\beta}(p) \leftrightarrow e^{-2i\rho}|n_-]\langle n_+|, \qquad\qquad \bar\varepsilon_{-,\alpha\dot\beta}^*(p) \leftrightarrow e^{-2i\rho}|n_+\rangle[n_-|, \tag{4.47b}$$

$$\varepsilon_0^{*\dot\alpha\beta}(p) \leftrightarrow \frac{1}{m\sqrt{2}}\Big(|p_+]\langle p_+| - |p_-]\langle p_-|\Big), \quad \bar\varepsilon_{0,\alpha\dot\beta}^*(p) \leftrightarrow \frac{1}{m\sqrt{2}}\Big(|p_+\rangle[p_+| - |p_-\rangle[p_-|\Big), \tag{4.47c}$$

where the first four relations are straightforward to prove for each element using eq. (4.5) and the last two follow directly from $\varepsilon_0^\mu(p) = s^\mu = \frac{1}{m}(p_+^\mu - p_-^\mu)$. Note that $\varepsilon_i^{*\dot\alpha\beta}(p) = \varepsilon_i^{*\mu}(p)\tau_\mu^{\dot\alpha\beta} \neq (\varepsilon_i^{\dot\alpha\beta}(p))^*$.

We can rewrite the expressions in eq. (4.47) in an alternative four-vector form by contracting them with either $\bar\tau_{\beta\dot\alpha}^\mu$ or $\tau^{\mu,\dot\beta\alpha}$, e.g. $\varepsilon_+^{*\mu}(p) = \varepsilon_+^{*\dot\alpha\beta}(p)\bar\tau_{\beta\dot\alpha}^\mu = e^{2i\rho}|n_+]^{\dot\alpha}\langle n_-|^\beta\bar\tau_{\beta\dot\alpha}^\mu = e^{2i\rho}\langle n_-|^\beta\bar\tau_{\beta\dot\alpha}^\mu|n_+]^{\dot\alpha} = e^{2i\rho}\langle n_-|\bar\tau^\mu|n_+]$. All three polarization vectors can then also be expressed as:

$$\varepsilon_+^{*\mu}(p) = e^{2i\rho}[n_+|\tau^\mu|n_-\rangle \qquad\qquad = e^{2i\rho}\langle n_-|\bar\tau^\mu|n_+], \tag{4.48a}$$

$$\varepsilon_-^{*\mu}(p) = e^{-2i\rho}[n_-|\tau^\mu|n_+\rangle \qquad\qquad = e^{-2i\rho}\langle n_+|\bar\tau^\mu|n_-], \tag{4.48b}$$

$$\varepsilon_0^{*\mu}(p) = \frac{1}{m\sqrt{2}}\Big([p_+|\tau^\mu|p_+\rangle - [p_-|\tau^\mu|p_-\rangle\Big) = \frac{1}{m\sqrt{2}}\Big(\langle p_+|\bar\tau^\mu|p_+] - \langle p_-|\bar\tau^\mu|p_-]\Big). \tag{4.48c}$$

20

4.3.2 In The General Light-like Decomposition

In the general decomposition the $(+, 0, -)$ indices do not refer to helicity but rather to the spin along the spatial part of the spin vector $s^\mu = \frac{p^\mu}{m} - \frac{m}{p \cdot q} q^\mu = \frac{1}{m}\left(p^{\flat\mu} - \alpha q^\mu\right)$, in the same way as for the generally decomposed Dirac spinors. These new relations look like

$$\varepsilon_+^{*\dot\alpha\beta}(p) \leftrightarrow \frac{|p^\flat]\langle q|}{\langle qp^\flat\rangle}, \qquad\qquad \bar\varepsilon_{+,\alpha\dot\beta}^*(p) \leftrightarrow \frac{|q\rangle[p^\flat|}{\langle qp^\flat\rangle}, \tag{4.49a}$$

$$\varepsilon_-^{*\dot\alpha\beta}(p) \leftrightarrow \frac{|q]\langle p^\flat|}{[p^\flat q]}, \qquad\qquad \bar\varepsilon_{-,\alpha\dot\beta}^*(p) \leftrightarrow \frac{|p^\flat\rangle[q|}{[p^\flat q]}, \tag{4.49b}$$

$$\varepsilon_0^{*\dot\alpha\beta}(p) \leftrightarrow \frac{1}{m\sqrt 2}\Big(|p^\flat]\langle p^\flat| - \alpha|q]\langle q|\Big), \quad \bar\varepsilon_{0,\alpha\dot\beta}^*(p) \leftrightarrow \frac{1}{m\sqrt 2}\Big(|p^\flat\rangle[p^\flat| - \alpha|q\rangle[q|\Big), \tag{4.49c}$$

and

$$\varepsilon_+^{*\mu}(p) = \frac{[p^\flat|\tau^\mu|q\rangle}{\langle qp^\flat\rangle} \qquad\qquad = \frac{\langle q|\bar\tau^\mu|p^\flat]}{\langle qp^\flat\rangle}, \tag{4.50a}$$

$$\varepsilon_-^{*\mu}(p) = \frac{[q|\tau^\mu|p^\flat\rangle}{[p^\flat q]} \qquad\qquad = \frac{\langle p^\flat|\bar\tau^\mu|q]}{[p^\flat q]}, \tag{4.50b}$$

$$\varepsilon_0^{*\mu}(p) = \frac{1}{m\sqrt 2}\Big([p^\flat|\tau^\mu|p^\flat\rangle - \alpha[q|\tau^\mu|q\rangle\Big) = \frac{1}{m\sqrt 2}\Big(\langle p^\flat|\bar\tau^\mu|p^\flat] - \alpha\langle q|\bar\tau^\mu|q]\Big), \tag{4.50c}$$

where at least by looking at the form of the Weyl spinors it is easy to see how these relations reduce to the eigenvalue decomposition relations in eq. (4.47) and eq. (4.48) in the special case where $p^\flat \to \lambda_+ n_+$ and $q \to n_-$. The positive and negative spin polarization vectors are of similar form to the massless polarization vectors in eq. (3.21), and in the massless limit $p^\flat \to p$ and q becomes a reference momentum instead of defining a spin axis so that the indices again refer to helicity.

5 Massive and Electroweak Chirality-Flow Rules

Now that we have the pieces needed for calculations that include massive particles in a convenient form, let us move to the diagrammatic level. One large difference between the massless and the massive case is in the relation between helicity and chirality. In the massless case, helicity and chirality are bound together in a one-to-one relation, so that only one chirality contributes to a certain helicity for a fermion. In the massive case, however, helicity and chirality are not bound together, and both chiral parts contribute to a specific helicity. This means that most[1] massive cases have a greater number of chirality-flow diagrams that contribute to a certain helicity configuration.

---

[1] One exception is with diagrams containing the ffW-vertex, since the chiral nature of the weak interaction only allows one type of chirality-flow for this vertex.

The massive fermion propagators carry an additional mass term which contributes to an increase of possible chirality-flow diagrams, and the fermion legs will have both chiral parts contributing to a certain helicity which also increases the number of possible chirality-flow diagrams. However, the massive boson propagators and external legs will not contribute to an increase of diagrams; the propagators will only have their denominators changed which do not alter the spinor contractions, and the possibility of a boson leg with longitudinal polarization also does not change the structure of the spinor contractions. We will also include the W, Z, and Higgs boson vertices to the chirality-flow formalism. The vertices can rather easily be written as chirality-flow diagrams using what we know from the massless case by examining their Lorentz index structure.

5.1   Massive Fermion Propagator

The denominator of the fermion propagator is trivial in the massive case. We simply replace p^2 with $p^2 - m^2$ and since the denominator is not related to the chirality-flow itself that is all we need to do. The numerator, however, contains $\not{p}_\gamma + m_f$ which in the chiral basis can be split into four parts so that for the entire propagator we have:

$$
\xleftarrow{\quad p \quad} \;=\; \frac{i(\not{p}_\gamma + m_f)}{p^2 - m_f^2} \;=\; \frac{i}{p^2 - m_f^2} \begin{pmatrix} m_f & \not{p}_\sigma \\ \bar{\not{p}}_{\bar\sigma} & m_f \end{pmatrix}
$$

$$
\leftrightarrow \frac{i}{p^2 - m_f^2} \begin{pmatrix} m_f \delta^{\dot\alpha}{}_{\dot\beta} & \sqrt{2}p^{\dot\alpha\beta} \\ \sqrt{2}\bar{p}_{\alpha\dot\beta} & m_f \delta_\alpha{}^\beta \end{pmatrix} \;=\; \frac{i}{p^2 - m_f^2} \begin{pmatrix} m_f \overset{p}{\underset{\dot\alpha \quad\quad \dot\beta}{\dashrightarrow}} & \overset{p}{\underset{\dot\alpha \quad\quad \beta}{\dashrightarrow\!\bullet\!\rightarrow}} \\ \underset{\alpha \quad\quad \dot\beta}{\overset{p}{\rightarrow\!\bullet\!\dashrightarrow}} & m_f \underset{\alpha \quad\quad \beta}{\longrightarrow} \end{pmatrix} , \quad (5.1)
$$

where in the final step we use the index structure to form a diagrammatic interpretation. The Kronecker deltas on the diagonal we have seen before in eq. (3.4). They connect the two relevant ends without flipping the chirality, as opposed to what we have seen the off-diagonal elements do. The off-diagonal elements, $\not{p}_\sigma$ and $\bar{\not{p}}_{\bar\sigma}$, can be used in the same way diagrammatically as in the massless case, except for the fact that they may contain momenta p_i where $p_i^2 \neq 0$, which need to be decomposed to two terms when written as products of Weyl spinors.

A simple example of a generic diagram with a fermion propagator is one with two fermion legs and two vector boson legs, shown in fig. 3, where all labels have been omitted for clarity. If the fermions are massive, so that both chiralities contribute to a specific helicity for that particle, four different chirality-flow diagrams will contribute to a specific helicity configuration for the entire Feynman diagram, shown in fig. 4. In this figure we can see the different components of the fermion propagator in eq. (5.1), in each of the four diagrams. For a given helicity configuration in the massless case, only one of the two diagrams on the left in fig. 4 survives, as both diagrams on the right always come with a factor of the
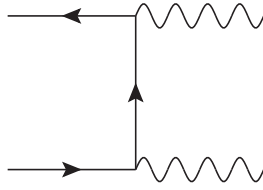
Figure 3: A Feynman diagram without particle labels.
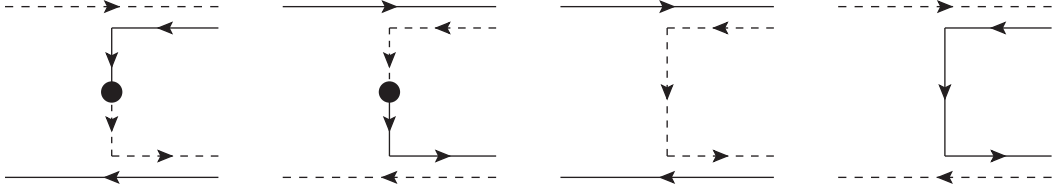
Figure 4: Four different types of chirality-flow diagrams that contribute to amplitudes for the type of Feynman diagram shown in fig. 3.

mass and therefore vanish in the massless case. Which of the two diagrams on the left that remain non-zero if $m_f = 0$ depends on the helicity of the fermions, because in the massless case only one chirality contributes to a specific helicity.

5.2 Massive Fermion Legs

For a massless fermion, only one of the two chiral parts of its Dirac spinor contributes for a specific helicity. A single $ff\gamma$-vertex may in the massless case look like this:

$$\leftrightarrow ie\sqrt{2} \qquad (5.2)$$

where we have a regular Feynman diagram on the left and its corresponding chirality-flow diagram on the right. The vector boson has been written as double lines in the chirality-flow diagram that can directly be contracted with another vertex or a polarization vector.

For a massive fermion, however, both the left and right chiral parts of its Dirac spinor contribute for a specific helicity. In the massive case the $ff\gamma$-vertex splits into two different types of chirality-flow:

$$\leftrightarrow ie\sqrt{2}\left[\;\; + \;\;\right]. \qquad (5.3)$$

23

We can see where this relation comes from by looking at the same expression in algebraic form:

$$\bar{u}_+(k)\left(ie\gamma^\mu\right)v_-(p) = ie\begin{pmatrix}k_{+,\dot\alpha} & -k_-^\alpha\end{pmatrix}\begin{pmatrix}0 & \sqrt{2}\tau^{\mu,\dot\alpha\beta}\\ \sqrt{2}\bar\tau^\mu_{\alpha\dot\beta} & 0\end{pmatrix}\begin{pmatrix}p_-^{\dot\beta}\\ p_{+,\beta}\end{pmatrix}$$
$$= ie\sqrt{2}\left[k_{+,\dot\alpha}\tau^{\mu,\dot\alpha\beta}p_{+,\beta} + (-k_-^\alpha)\bar\tau^\mu_{\alpha\dot\beta}p_-^{\dot\beta}\right], \tag{5.4}$$

where the spinors for the two helicities are taken from eq. (4.35). The two chirality-flow diagrams in eq. (5.3) are the diagrammatic interpretations of the two terms in square brackets in eq. (5.4).

When $m = 0$, the eigenvalues $\lambda_- = p_0 - |\mathbf{p}|$ are zero for both momenta k and p, so both k_- and p_- are zero since they are both proportional to $\sqrt{\lambda_-}$. If no helicities have been specified for the legs, there is no way to tell which part disappears when $m = 0$. If specific helicities have been given, however, it is possible to see which part goes away in the massless limit for any type of decomposition since both λ_- and $\alpha = \frac{p^2}{2p\cdot q}$ equal zero when $m = 0$.

A different example we can use is:

$$\tag{5.5}$$

where now both fermions have positive helicity. This helicity configuration does contribute in the massive case but not in the massless case, because both p_- in the left term and k_- in the right term will be zero in the massless case. The chirality-flow diagrams help us in this case to see instantly that this helicity configuration does not contribute in the massless case.

5.3 Electroweak Vertices

All the vertices discussed in this section are taken from [12]. The source includes Faddeev-Popov ghosts, counterterms, and the three additional scalar fields from the Higgs doublet, but we ignore these for now. We also ignore gluons in this section as they have already been dealt with in [1].

The vector particle vertex $V\bar{f}f$ can in a general way be written as

$$= ie\gamma^\mu(C_L P_L + C_R P_R), \tag{5.6}$$

where P_L and P_R are the chiral projection operators from eq. (2.7), and C_L and C_R are constants that depend on the specific particles involved in the vertex. We can write this out in matrix form and write the τ-matrices as chirality-flow diagrams:

$$\mu \quad = ie\gamma^\mu(C_L P_L + C_R P_R) = ie\sqrt{2}\begin{pmatrix} 0 & C_R\tau^\mu \\ C_L\bar{\tau}^\mu & 0 \end{pmatrix} \tag{5.7}$$

$$\leftrightarrow ie\sqrt{2}\begin{pmatrix} 0 & C_R \\ & \\ C_L & 0 \end{pmatrix} \tag{5.8}$$

If we again look at eq. (5.4) but for an arbitrary electroweak vector boson instead of a photon, we instead get:

$$\bar{u}_+(k)\left[ie\gamma^\mu(C_L P_L + C_R P_R)\right]v_-(p) = ie\sqrt{2}\begin{pmatrix} k_{+,\dot\alpha} & -k_-^\alpha \end{pmatrix}\begin{pmatrix} 0 & C_R\tau^{\mu,\dot\alpha\beta} \\ C_L\bar{\tau}^\mu_{\alpha\dot\beta} & 0 \end{pmatrix}\begin{pmatrix} p_-^{\dot\beta} \\ p_{+,\beta} \end{pmatrix}$$

$$=ie\sqrt{2}\left[C_R k_{+,\dot\alpha}\tau^{\mu,\dot\alpha\beta}p_{+,\beta} + C_L(-k_-^\alpha)\bar{\tau}^\mu_{\alpha\dot\beta}p_-^{\dot\beta}\right]. \tag{5.9}$$
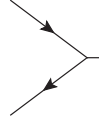
From this we see that C_L is connected to the left-chiral part of an *outgoing anti-particle* ($p_-^{\dot\beta}$ in this case). If we were to consider incoming particles instead, C_L would be connected to the left-chiral part of an *incoming particle*. This is consistent with the fact that W-bosons only couple to the left-chiral parts of *incoming particles*, since $C_R = 0$ for W-bosons, as can be seen in table 1.

Vertex	C_L	C_R
$\gamma\bar{f}f$	$-Q_f$	$-Q_f$
$Z\bar{f}f$	$\frac{I^3_{W,f}-Q_f\sin^2\theta_W}{\sin\theta_W\cos\theta_W}$	$-\frac{\sin\theta_W}{\cos\theta_W}Q_f$
$W^+\bar{u}_i d_j$	$\frac{1}{\sqrt{2}\sin\theta_W}(V_{CKM})_{ij}$	0
$W^-\bar{d}_i u_j$	$\frac{1}{\sqrt{2}\sin\theta_W}(V_{CKM})^\dagger_{ij}$	0
$W^+\bar{\nu}_i l_j$	$\frac{1}{\sqrt{2}\sin\theta_W}\delta_{ij}$	0
$W^-\bar{l}_i \nu_j$	$\frac{1}{\sqrt{2}\sin\theta_W}\delta_{ij}$	0

Table 1: The values of C_L and C_R for the different $V\bar{f}f$-vertices.

The scalar particle vertex $S\bar{f}f$ can be written in a similar way to the $V\bar{f}f$-vertex, by
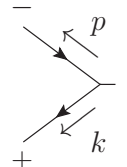
simply excluding γ^μ:

$$\text{---} = ie\,(C_L P_L + C_R P_R). \tag{5.10}$$
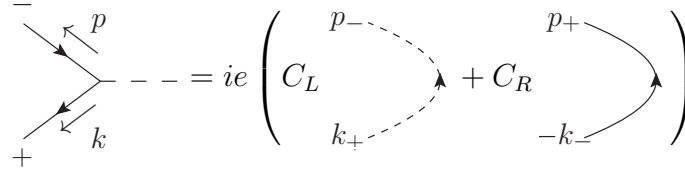
The only vertex relevant for us right now is the Higgs vertex $H\bar{f}f$ where $C_L = C_R = -\frac{m_f}{2\sin\theta_W M_W}$. We could also insert a different scalar field from the Higgs doublet and get different values for C_L and C_R, but as mentioned in the beginning of this section we ignore these for now.

As an example, let us treat the two fermions as outgoing particles with assigned helicities and write the diagram in algebraic form:

$$\text{---} = \bar{u}_+(k)\,ie\,(C_L P_L + C_R P_R)\,v_-(p)$$

$$= ie\begin{pmatrix} k_{+,\dot\alpha} & -k_-^\alpha \end{pmatrix}(C_L P_L + C_R P_R)\begin{pmatrix} p_-^{\dot\alpha} \\ p_{+,\alpha} \end{pmatrix}$$

$$= ie\left(C_L k_{+,\dot\alpha}p_-^{\dot\alpha} + C_R\left(-k_-^\alpha\right)p_{+,\alpha}\right) \tag{5.11}$$
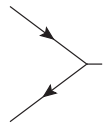
We see that scalar particles connect Weyl spinors of the same index type directly at the vertex. These spinor contractions can be interpreted with chirality-flow diagrams,

$$\text{---} = ie\left(C_L \begin{array}{c} p_- \\ k_+ \end{array} + C_R \begin{array}{c} p_+ \\ -k_- \end{array} \right) \tag{5.12}$$

where the scalar line has been removed from the chirality-flow diagrams as it does not add any additional information at this level.

The contractions in eq. (5.12) imply a certain structure for the vertex:

$$\text{---} = ie\,(C_L P_L + C_R P_R)$$

$$= ie\begin{pmatrix} C_L & 0 \\ 0 & C_R \end{pmatrix} = ie\begin{pmatrix} C_L & & 0 \\ & & \\ 0 & & C_R \end{pmatrix}, \tag{5.13}$$

26

The vertices consisting of three and four vector bosons have the same form as the gluon vertices, but with different constants that can be found in table 2. We have already seen from eq. (3.18) and eq. (3.11) that $g_{\mu\nu}$ and p_μ can be put into a diagrammatic form:

$$g_{\mu\nu} \leftrightarrow \;\overline{}\;\; \text{and} \quad \sqrt{2}p_\mu \leftrightarrow \;\; p \; \bullet\!\!\!\diagdown\!\!\!\text{------} \;. \tag{5.14}$$

If we do this for both vertices we get

$$= -ieC_{VVV}\left[g_{\mu_1\mu_2}(p_1-p_2)_{\mu_3} + g_{\mu_2\mu_3}(p_2-p_3)_{\mu_1} + g_{\mu_3\mu_1}(p_3-p_1)_{\mu_2}\right]$$

$$(5.15)$$

and

$$= ie^2 C_{VVVV}\left(2g_{\mu_1\mu_3}g_{\mu_4\mu_2} - g_{\mu_1\mu_2}g_{\mu_3\mu_4} - g_{\mu_1\mu_4}g_{\mu_2\mu_3}\right)$$

$$(5.16)$$

There are three additional vertices that contain factors in the form of $g_{\mu\nu}$ or p_μ: VVS (vector-vector-scalar), $VVSS$, and VSS. All VSS interactions involve at least one non-Higgs electroweak scalar and the details around these are left out of this thesis, but the vertex is still included to show that interactions of this type can also be put into diagrammatic form. We can use eq. (5.14) to put these three diagrams into diagrammatic form as

Vertex	C_{vertex}
$\gamma W^+ W^-$	1
$Z W^+ W^-$	$-\frac{\cos\theta_W}{\sin\theta_W}$
$W^+ W^- W^+ W^-$	$\frac{1}{\sin^2\theta_W}$
$W^+ Z W^- Z$	$-\frac{\cos^2\theta_W}{\sin^2\theta_W}$
$W^+ \gamma W^- Z$	$\frac{\cos\theta_W}{\sin\theta_W}$
$W^+ \gamma W^- \gamma$	-1
HHH	$-\frac{3}{2\sin\theta_W}\frac{M_H^2}{M_W}$
$HHHH$	$-\frac{3}{2\sin^2\theta_W}\frac{M_H^2}{M_W^2}$
$H W^+ W^-$	$\frac{M_W}{\sin\theta_W}$
HZZ	$\frac{M_W}{\sin\theta_W\cos^2\theta_W}$
$W^+ W^- HH$	$\frac{1}{2\sin^2\theta_W}$
$ZZHH$	$\frac{1}{2\sin^2\theta_W\cos^2\theta_W}$

Table 2: Values of the factor C_{vertex} for the different boson vertices.

well:

$$ = ieC_{VVS}g_{\mu_1\mu_2} \qquad \leftrightarrow ieC_{VVS} \tag{5.17}$$

$$ = ie^2 C_{VVSS}g_{\mu_1\mu_2} \qquad \leftrightarrow ie^2 C_{VVSS} \tag{5.18}$$

$$ = ieC_{VSS}\left(k_1 - k_2\right)_\mu \leftrightarrow ieC_{VSS}\frac{1}{\sqrt{2}} \tag{5.19}$$

The final vertices that need to be dealt with are the simplest. The SSS and $SSSS$ vertices,

$$ = ieC_{SSS} \quad \text{and} \quad = ie^2 C_{SSSS}, \tag{5.20}$$

do not contain any Lorentz factors and therefore do not affect the chirality-flow structure. Any scalar line in a Feynman diagram can be completely ignored when drawing the relevant chirality-flow diagrams, as long as the multiplicative factors from scalar interactions are included.

Vertices		
Feynman	Dirac	Chirality-flow
	$ie\gamma_\mu(C_L P_L + C_R P_R)$	$ie\sqrt{2}\left(C_L \quad + C_R \right)$
	$ie(C_L P_L + C_R P_R)$	$ie\left(C_L \quad + C_R \right)$
	$ieC_{VVS}\,g_{\mu_1\mu_2}$	ieC_{VVS}
	$ieC_{VSS}(p_1 - p_2)_\mu$	$ieC_{VSS}\dfrac{1}{\sqrt{2}}$
	ieC_{SSS}	ieC_{SSS}
	$-ieC_{VVV}\left[g_{\mu_1\mu_2}(p_1-p_2)_{\mu_3} + g_{\mu_2\mu_3}(p_2-p_3)_{\mu_1} + g_{\mu_3\mu_1}(p_3-p_1)_{\mu_2}\right]$	$-ieC_{VVV}\dfrac{1}{\sqrt{2}}\left(\quad + \quad + \quad \right)$
	$ie^2 C_{SSSS}$	$ie^2 C_{SSSS}$
	$ie^2 C_{VVSS}\,g_{\mu_1\mu_2}$	$ie^2 C_{VVSS}$
	$ie^2 C_{VVVV}\left(2g_{\mu_1\mu_3}g_{\mu_4\mu_2} - g_{\mu_1\mu_2}g_{\mu_3\mu_4} - g_{\mu_1\mu_4}g_{\mu_2\mu_3}\right)$	$ie^2 C_{VVVV}\left(2 \quad - \quad - \quad \right)$

Table 3: Chirality-flow rules for the different electroweak vertices. The factors of $C_{L/R}$ and C_{vertex} can be found in table 1 and table 2, respectively.

6 Massive and Electroweak Diagram Examples

We will now look at some examples of Feynman diagram calculations using the chirality-flow method. We being with an example used earlier in fig. 2, but now for massive fermions, shown in fig. 5. We remind the reader that in our *Feynman diagrams*, helicities are denoted by *superscript* $+$ and $-$ signs, and in the following *chirality-flow diagrams*, the eigenvalue decomposition Weyl spinors are denoted by *subscript* $+$ and $-$ signs. In this diagram and all others in this section, all particles are considered outgoing.
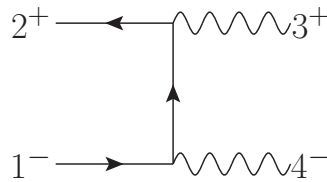
Figure 5: A $ff\gamma\gamma$ diagram with a given helicity configuration. The fermions are considered massive.
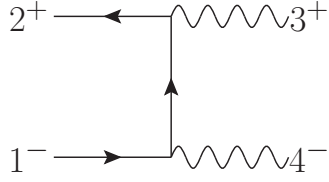
We begin by collecting a factor of $ie\sqrt{2}(-Q_f)$ from each of the two vertices, a factor of $\dfrac{i}{(p_2 + p_3)^2 - m_f^2}$ from the fermion propagator, and a factor of $\dfrac{1}{\langle r_3 3\rangle\,[4 r_4]}$ from the two polarization vectors. We then go through all the possible chirality-flow diagrams for this Feynman diagram, and add the respective Weyl spinor labels to all of them. The only chirality-flow diagrams possible for this Feynman diagram are shown in fig. 4. Fermion number 2 is a positive helicity outgoing particle and fermion number 1 is a negative helicity outgoing anti-fermion. These can be represented by the Dirac spinors

$$\overline{u}^+(p_2) = \begin{pmatrix} [2_+|_{\dot\alpha} & -\langle 2_-|^{\alpha} \end{pmatrix} \quad \text{and} \quad v^-(p_1) = \begin{pmatrix} |1_-]^{\dot\alpha} \\ |1_+\rangle_{\alpha} \end{pmatrix}, \tag{6.1}$$

expressed in terms of the eigenvalue decomposition Weyl spinors, where indices have been added to clearly show what is dotted and what is undotted. We use these to add the dotted spinors to the dotted lines and the undotted spinors to the undotted lines for particles 1 and 2. Particle number 3 is a positive helicity photon, which means that the dotted lines are given the physical momentum label 3 and the undotted lines are given the reference momentum label r_3; the opposite applies for particle number 4 since it has negative helicity. Through the propagator we have the momentum $p_2 + p_3$ so the momentum dot in the chirality-flow diagrams are simply given the label $2 + 3$. The diagrams without a momentum dot in the propagator come with a factor of m_f.

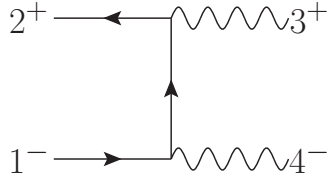After some practice with the chirality-flow method it is possible to put these pieces together

almost immediately, so that

$$
\begin{aligned}
&\quad = ie\sqrt{2}(-Q_f)\frac{i}{(p_2+p_3)^2-m_f^2}ie\sqrt{2}(-Q_f)\frac{1}{\langle r_3 3\rangle [4 r_4]} \cdot
\end{aligned}
$$

$$
\tag{6.2}
$$

At this stage we are in principle done with the calculation since every line corresponds directly to a Weyl spinor contraction. However, for clarity we will also write this expression in algebraic form:

$$
= ie\sqrt{2}(-Q_f)\frac{i}{(p_2+p_3)^2-m_f^2}ie\sqrt{2}(-Q_f)\frac{1}{\langle r_3 3\rangle [4 r_4]} \cdot
$$

$$
\cdot \bigg[[2_+ 3] \langle r_3| \Big(|2_+\rangle[2_+| + |2_-\rangle[2_-| + |3\rangle[3| \Big) |r_4] \langle 4 1_+\rangle
$$

$$
- \langle 2_- r_3\rangle [3| \Big(|2_+]\langle 2_+| + |2_-]\langle 2_-| + |3]\langle 3| \Big) |4] [r_4 1_-]
$$

$$
+ m_f [2_+ 3] \langle r_3 4\rangle [r_4 1_-] - m_f \langle 2_- r_3\rangle [3 r_4] \langle 4 1_+\rangle \bigg]
$$

$$
\tag{6.3}
$$

As a check, it is also possible to arrive at the same expression as in eq. (6.3) without the use of chirality-flow diagrams, using standard Feynman rules and spinor-helicity methods, which has been done for this and the following examples. This process, however, is slower than using the chirality-flow method.

When the mass goes to zero both Weyl spinors 1_- and 2_- also go to zero because they are proportional to $\sqrt{\lambda_{i,-}} = \sqrt{p_i^0 - |\mathbf{p}_i|}$ which is zero when $p_i^2 = 0$. This means that the only

surviving chirality-flow diagram in the massless case is the first diagram out of the four above, which is exactly the same as the diagram in the earlier massless example in fig. 2.

Another example we can use is a diagram relevant for associated Higgs production, shown in fig. 6. The superscript 0 in 4^0 refers to the longitudinal polarization which is a possibility
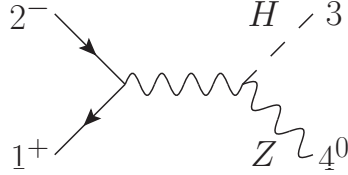

Figure 6: An associated Higgs production diagram with a given helicity configuration.

for any massive vector boson. We again collect all the factors from vertices, propagators, and polarization vectors, we draw the only two possible chirality-flow diagrams, and finally use the Dirac spinor solutions to place the Weyl spinors in their correct positions. The result is

$$
= ie\sqrt{2}\frac{-i}{(p_1 + p_2)^2 - m_Z^2}ie\frac{m_W}{\sin\theta_W \cos^2\theta_W}\frac{1}{m\sqrt{2}}\cdot
$$

$$
\cdot\left[C_L \quad\quad + C_R \quad\quad \right], \tag{6.4}
$$

which can also be written as

$$
= ie\sqrt{2}\frac{-i}{(p_1 + p_2)^2 - m_Z^2}ie\frac{m_W}{\sin\theta_W \cos^2\theta_W}\frac{1}{m\sqrt{2}}\cdot
$$

$$
\cdot\left[-C_L\langle 1_-|\Big(|4_+\rangle[4_+| - |4_-\rangle[4_-|\Big)|2_-] + C_R[1_+|\Big(|4_+]\langle 4_+| - |4_-]\langle 4_-|\Big)|2_+\rangle \right] \tag{6.5}
$$

As a final example, we will calculate a more complicated diagram, shown in fig. 7. In the same way as before, we collect the factors coming from vertices and propagators, but we do not immediately write down all possible *complete* chirality-flow diagrams. Instead, we write them as products of *partial* chirality-flow diagrams by cutting the vector boson that connects the two fermion lines. This allows us to more easily find all possible chirality-flow
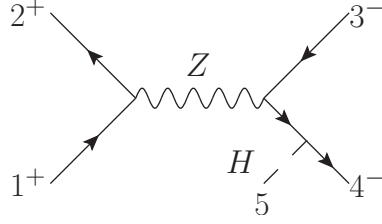
32

Figure 7: A Higgs production diagram with a given helicity configuration. This Feynman diagram can be written as a sum of eight chirality-flow diagrams.

diagrams and helps us to keep better track of the arrow directions to avoid sign mistakes that may appear when there are an odd number of spinor contractions. The result is:

$$
\begin{aligned}
&\quad = ie\sqrt{2}\frac{-i}{(p_1+p_2)^2 - m_Z^2}ie\sqrt{2} \ \times \\
\end{aligned}
$$

$$
\times \frac{i}{(p_4+p_5)^2 - m_4^2}ie\left(-\frac{m_f}{2\sin\theta_W m_W}\right)\left[C_{L,12} \quad + C_{R,12} \quad \right] \times
$$

$$
\times \left[C_{L,34} \quad 4+5 \ + C_{L,34}m_4 \quad + C_{R,34} \quad 4+5 \ + C_{R,34}m_4 \quad \right]
\tag{6.6}
$$

Some pairs of partial diagrams above can be connected instantly by gluing together the two line types, undotted to undotted and dotted to dotted, because the arrow direction is the same. In other pairs the arrow direction does not immediately match, but it is possible to flip the direction of the arrows in one of the two partial diagrams. A simple example of this is

$$
\tag{6.7}
$$

which can also be written as

$$
\langle i|\bar{\tau}^\mu|j] = [j|\tau^\mu|i\rangle.
\tag{6.8}
$$

33

A slightly more complicated example which also introduces a minus sign when the arrow direction is flipped is

$$\text{(6.9)}$$

which can also be written as

$$\langle j|\bar{\not{p}}\tau^\mu|i\rangle = -\langle i|\bar{\tau}^\mu\not{p}|j\rangle. \tag{6.10}$$

Changing the arrow direction of a single line always introduces a minus sign, which is why an even number of arrow direction flips (as in the first example) does not give a minus sign, but an odd number of flips (as in the second example) does give a minus sign; in the second example the momentum dot divides a line into two lines.

The final result after flipping the required arrow directions and gluing the diagrams together is

$$= ie\sqrt{2}\,\frac{-i}{(p_1+p_2)^2 - m_Z^2}\,ie\sqrt{2}\,\frac{i}{(p_4+p_5)^2 - m_4^2}\,ie\left(-\frac{m_f}{2\sin\theta_W m_W}\right)\times$$

$$\times\left[C_{L,12}C_{L,34}\quad + C_{R,12}C_{L,34}\right.$$

$$C_{L,12}C_{L,34}m_4 \quad + C_{R,12}C_{L,34}m_4$$

$$C_{L,12}C_{R,34} \quad + C_{R,12}C_{R,34}$$

$$\left. C_{L,12}C_{R,34}m_4 \quad + C_{R,12}C_{R,34}m_4\right] \tag{6.11}$$

34

If the Z-boson propagator had instead been a W-boson, all factors of C_R would have been zero, which means that only 2 out of the 8 diagrams would survive.

7 Conclusion and Outlook

In this thesis we have found a way to extend the chirality-flow method from massless QED and QCD to the full standard model. In the examples shown we have seen that helicity amplitudes are easy and quick to calculate using the chirality-flow method. Using this method it is possible to go from Feynman diagram to a complex number with very little effort.

The electroweak vector bosons can be treated similarly to photons and gluons, with the addition of longitudinal polarization for massive vector bosons. Scalar particles have no Lorentz structure and are therefore not assigned any chirality-flow lines. For massive fermions, both left- and right-chiral parts contribute to a specific helicity eigenstate which increases the number of chirality-flow diagrams that contribute to a certain helicity amplitude. This means that massive helicity amplitudes can effectively be broken down into a sum of chirality-flow diagrams that can be treated individually using massless methods. We have also seen that the W-boson can drastically simplify expressions, by reducing the number of allowed chirality-flow diagrams.

There are still some interesting topics that are worthy of further study. In the examples in this thesis we have used the eigenvalue decomposition for pedagogical and aesthetic reasons, but it is possible that the general light-like decomposition may be preferable in many practical cases. It would be useful to find ways to choose the reference momentum such that we maximize symmetry, cancellation, or computer efficiency, perhaps by only looking at the chirality-flow diagrams. Loop calculations have been ignored for the moment, but it would be favourable if these could also be included in the chirality-flow method. Finally, it may also be interesting to try to include extensions of the standard model, e.g. the Two-Higgs-doublet model (2HDM) [13], and higher representations of the Lorentz group into the chirality-flow method. For the higher representations, spin-$\frac{3}{2}$ particles in the Weyl-van-der-Waerden formalism can be found in [14], and spinor techniques for spin-2 gravitons in [15].

References

[1] A. Lifson, C. Reuschle and M. Sjodahl, *The chirality-flow formalism*, 2003.05877.

[2] H. Elvang and Y.-t. Huang, *Scattering amplitudes*, 1308.1697.

[3] L. J. Dixon, *A brief introduction to modern amplitude methods*, 1310.5353.

[4] S. Weinzierl, *Automated calculations for multi-leg processes*, *PoS* **ACAT** (2007) 005 [`0707.3342`].

[5] L. Dixon, *Calculating scattering amplitudes efficiently*, `hep-ph/9601359`.

[6] A. Zee, *Quantum field theory in a nutshell*, Nutshell handbook. Princeton Univ. Press, Princeton, NJ, 2003.

[7] H. K. Dreiner, H. E. Haber and S. P. Martin, *Two-component spinor techniques and Feynman rules for quantum field theory and supersymmetry*, *Physics Reports* **494** (2010) 1–196.

[8] J. Schwichtenberg, *Physics from symmetry*, Undergraduate Lecture Notes in Physics. Springer International Publishing, Cham, 2018, 10.1007/978-3-319-66631-0.

[9] S. Dittmaier, *Weyl-van der Waerden formalism for helicity amplitudes of massive particles*, *Phys. Rev. D* **59** (1998) 016007 [`hep-ph/9805445`].

[10] C. Schwinn and S. Weinzierl, *Born amplitudes in QCD from scalar diagrams*, *Nuclear Physics B - Proceedings Supplements* **164** (2007) 54–59.

[11] R. Kleiss and W. Stirling, *Spinor techniques for calculating $pp \rightarrow W^{\pm}/Z^0 + jets$*, *Nucl. Phys. B* **262** (1985) 235.

[12] A. Denner, *Techniques for the calculation of electroweak radiative corrections at the one-loop level and results for W-physics at LEP200*, `0709.1075`.

[13] G. Branco, P. Ferreira, L. Lavoura, M. Rebelo, M. Sher and J. P. Silva, *Theory and phenomenology of two-Higgs-doublet models*, *Phys. Rept.* **516** (2012) 1 [`1106.0034`].

[14] S. Novaes and D. Spehler, *Weyl-van der Waerden spinor technique for spin 3/2 fermions*, *Nucl. Phys. B* **371** (1992) 618.

[15] H. Cho and K. Ng, *Spinor technique in graviton scattering processes*, *Phys. Rev. D* **47** (1993) 1692.